IN THE UNITED STATES PATENT AND TRADEMARK OFFICE

Examiner	:	Falk, Anne Marie
Art Unit	:	1632
Applicants	:	Klein et al.
Serial No.	:	09/780,041
Docket No.	:	UF-10293
Filed	:	02/09/2001
For	:	Human Disease Modeling Using Somatic Gene Transfer

Assistant Commissioner for Patents
Washington, D.C. 20231

DECLARATION OF RONALD KLEIN, PhD.

I, Ronald Klein, Ph.D. hereby declare and say as follows:

THAT, I am employed as an assistant professor at Louisiana State University Health Sciences Center, Shreveport, LA.;

THAT, I earned my Ph.D. in Pharmacology in 1995, from University of Colorado Health Sciences Center, Denver, CO, a copy of my curriculum vitae is attached hereto as Exhibit A;

THAT, I am one of the above-named Applicants and inventors of the subject matter described and claimed in the above-identified patent application;

THAT, by virtue of my educational and employment background, my attendance at seminars, my ongoing research, my continuing review of scientific periodicals and journals, and through correspondence with professional colleagues, I am aware of the level of skill of one ordinarily skilled in the art of neuroscience, pharmacology, and gene therapy;

THAT, I have studied the application Serial No. 09/780/041 and all office actions which have been issued during prosecution of this application (including cited

references), as well as all responses which have been filed on the Applicants' behalf, and being thus duly qualified declare as follows:

1. The Patent Office questions whether the somatic gene transfer methods taught in the specification and claimed in the subject application will achieve the desired phenotype in animals other than the rat. The office action cites a number of references to allege that *in vivo* genetic modifications is unpredictable. In particular, the Patent Office questions whether the phenotype of neuronal pathology that is produced in rats could not be produced in other animals without undue experimentation. The Patent Office questions whether the claimed methods and compositions would produce a similar pathological profile in higher mammals other than rats, and even questions whether they would work in other rodents such as mice. See page 6 of Office Action dated 11/5/02.

2. As a preliminary matter, the neuronal pathways and neuroanatomy of rats, mice, and higher mammals such as dogs and monkeys is well characterized. Techniques for delivering substances for specific areas of the brains in higher animals is well established. The characteristics of the neuronal pathways in rats and higher animals that equate to the pathways involved in human neurological pathology is also well established. From a scientific point of view, there is no valid scientific reason to believe that the tau-containing vectors delivered to brains other than rat brains would not be expressed and not produce the same neuropathology that we have shown in rats. Certainly, given their closely similar neuroantaomy, one would expect that the neuropathology original shown to occur in rat brains would also occur in mice brain.

3. Indeed, I attach hereto a manuscript demonstrating that the delivery to mice brain of the same tau containing vectors shown to produce tau pathology in rat brain produced similar tau pathology in mice brain. Exhibit B, see Figure 4A-B. It is noted that the mice used in this study were doubly transgenic PS1/APP mice. However, the fact that the mice used in this study were transgenic PS1/APP mice should be of no consequence to the predictability of producing a tau-pathology in mice. We have shown that the pCB-Tau AAV vectors were successfully expressed in both rat and

mice brain. Furthermore, the expression of this vector produced a tau pathology in both rat and mice brain. This evidence clearly demonstrates that the Applicants of the present application were in possession of and enabled methods of producing models in mice as well as rats.

4. In addition, I attach an article (Kirik et al.; Exhibit C) which reports the results of implementing the somatic gene transfer techniques as taught in the subject application in primates. As you can see, AAV vectors containing the alpha-synuclein gene were introduced into the nigrostriatal neurons of adult marmosets. The article reports that the alpha-synuclein gene was expressed, and that this expression caused severe neuronal pathology, including alpha-synuclein- positive cytoplasmic inclusions and granular deposits; swollen, dystrophic, and fragmented neuritis, and shrunken and pyknotic, densely alpha-synuclein perikarya. While this study involved the introduction of the alpha-synuclein gene, and not a mutant tau gene, it nonetheless shows that the claimed methods are sound and would be expected to work in animals comprising the appropriate neural pathways. The fact that introduction of alpha-synuclein gene in marmosets produces neural pathology as predicted by the teachings of the subject application evidences the high likelihood that introduction of a mutant tau gene in animals other than rats would also produce tau pathology in those other animals. Certainly, I would expect that the tau pathology observed in rats and mice would be also be observed in higher mammals. The fact that the methods as presently claimed would equally work in both rats and mice is abundantly clear.

5. Furthermore, I include references which discuss various versions of mutated tau proteins that have been shown to be associated with a neurological condition. Exhibit D. In my opinion, it would be routine to substitute these other mutant tau proteins for the P301L mutant tau protein specifically described in the Examples section of the subject application, and used in the attached study. Furthermore, the expression of these other mutant tau proteins, and whether they produce the related neuropathology, in animal brain could be easily determined without undue experimentation.

6. The undersigned declares further that all statements made herein of his own knowledge are true and that all statements made on information in belief are believed to be true; and further that these statements were made with the knowledge that willful false statements in the like so made are punishable by fine or imprisonment, or both, under ' 1001 of title 18 of the U.S.C. and that such willful false statements made jeopardize the validity of the application or of any patent issuing thereon.

Further declarant sayeth naught.

Ronald Klein

Ronald Klein, Ph.D.

Aug. 1, 2003

Date

Exhibit A

Curriculum Vitae

RONALD LEE KLEIN, Ph.D.

ADDRESS Department of Pharmacology and Therapeutics, Box 33932
Louisiana State University Health Sciences Center-Shreveport
1501 Kings Highway
Shreveport, LA 71130-3932
(318) 675-7830; fax (318) 675-7857; klein@lsuhsc.edu

PERSONAL Born July 24, 1965 in Hackensack, NJ.

EDUCATION

Ph.D., Pharmacology; Date of graduation: May, 1995.
University of Colorado Health Sciences Center, Denver, CO.
Dissertation Title: Chronic and Acute Drug Actions on the Binding and Function of Native and Recombinant GABA–A Receptors.
Advisor: R. Adron Harris, Ph.D.

Bachelor of Arts; Date of graduation: May, 1987.
Hamilton College, Clinton, NY. Major: Psychobiology; Minor: Studio Art.

Pascack Valley High School, Hillsdale, NJ.
Outstanding Student in Latin Award 1981 and 1982.

PROFESSIONAL EXPERIENCE

Assistant Professor, 2002-present, Department of Pharmacology and Therapeutics, Louisiana State University Health Sciences Center-Shreveport.
Focus on gene targets of Alzheimer's and Parkinson's disease.

Assistant in Pharmacology, 1999-2002, Department of Pharmacology, University of Florida.
Postdoctoral Associate, 1995-1999, Department of Pharmacology, University of Florida.
Advisor: Edwin M. Meyer, Ph.D. (from 1995-2002)
Co-advisor: Nicholas Muzyczka, Ph.D. (from 1996-1998)
Investigations of gene transfer to the brain. Techniques: design and construction of plasmid DNAs, DNA sequencing, site-directed mutagenesis, construction of fusion protein cDNAs, quantitative-competitive PCR, preparation and characterization of recombinant adeno-associated virus, stereotaxic injections and lesions, locomotor behavior, passive-avoidance behavior, Morris water task, rotating rod behavior, confocal imaging of antigen-specific neurons and stereological morphometric analyses.

Graduate Student, 1989-1995. Department of Pharmacology, University of Colorado Health Sciences Center. Investigations of recombinant GABA-A receptor regulation by chronic drug treatments. Techniques: radioligand binding assays, GABA-A receptor functional assay (36-Cl uptake), northern, southern, and western blotting, PCR, electrophysiological recording from *Xenopus* oocytes, and transient transfection of mammalian cells.

Research Assistant, 1987-1989. Laboratory of Molecular and Cellular Neuroscience, Rockefeller University, New York, NY. Supervisor: Martin Bähler, Ph.D.; Lab Chief: Paul Greengard, Ph.D. Investigations of synaptic vescicle phosphoproteins. Techniques: western blotting, tissue culture, immunofluorescence, protein chemistry, purification and conjugation of antibodies.

Undergraduate Student, 1986-1987, Hamilton College, Clinton, NY. Independent research of testosterone levels and aggressive behavior in hamsters. Training in stereotaxic injections and electrophysiological recording.

AWARDS

PI, National Parkinson's Foundation, 10/1/03-9/30/04
"Gene transfer to the brain for novel comprehensive models of Parkinson's disease"
PI, The Society for Progressive Supranuclear Palsy, 11/1/03-10/31/04
"Aging effects and gene therapy in a novel nigrostriatal degeneration model"
PI, Eichler Award/The Parkinson's Disease Resource of NW Louisiana , 71/03-6/30/04
"Development of gene transfer vectors to study Parkinson's disease"
PI, Alzheimer's Association, NIRG-00-2270, 2000-2002.
"In vivo somatic gene transfer approaches to Alzheimer's disease therapeutics"
Co-I, NIH R01 NS37432 (E. Meyer PI), 1999-2002.
"AAV-mediated neurotrophic factor gene delivery to the brain"
Co-I, NIH P01 AG10485 (J. Simkins PI; M. King PI on Project 3), 8/99-7/04.
"AAV-mediated gene transfer for animal models of Alzheimer's disease"
NIH trainee 1995-1997. Training Grant T32 AGOO196.
NIH trainee 1989-1991. Training Grant T32 GMO7635.
Guest Researcher, Department of Organic Materials, National Institute of Advanced Industrial Science and Technology, Osaka, Japan, March, 2001.
Summer Institute in Japan 1995.
Division of International Programs, National Science Foundation,
Fujisawa Pharmaceutical Co., Ltd. in Tsukuba, Japan.
Student Research Forum Award in Molecular Biology 1993.
Department of Veteran's Affairs Performance Award 1993.
American Society for Pharmacology and Experimental Therapeutics
Travel Award 1993.

INVITED SEMINARS

University of Bristol, Bristol, UK, November 29, 2000. "Techniques for gene manipulation targeting and delivery in the nervous system" short course.
Institute for Protein Research, Osaka University, Osaka, Japan, March 16, 2001.
National Institute for Advanced Industrial Science & Technology, Osaka, Japan, July 22, 2002.
Nippon Medical School, Tokyo, Japan, July 26, 2002.
Jichi Medical School, Tochigi, Japan, July 29, 2002.

EDITOR

Methods vol. 28 (2002) Adeno-associated virus vectorology and gene therapy applications.

REVIEWER

Brain Research, Experimental Neurolog y, Molecular Therapy, Neurobiology of Disease
Alzheimer's Association
Association Francaise contre les Myopathies
NIH ad-hoc reviewer, Integrative, Cognitive, and Functional Neuroscience 1 (IFCN1) special emphasis panel, June 12, 2002.

BIBLIOGRAPHY

1. Bähler M., Cesura A.M., Fischer G., Kuhn H., Klein R.L., and M. DaPrada (1990) Serotonin organelles of rabbit platelets contain synaptophysin. *Eur. J. Biochem.* 194:825-829.

2. Bähler M., Klein R.L., Wang J.K., Benfenati F., and P. Greengard (1991) A novel synaptic vesicle-associated phosphoprotein: SVAPP-120. *J. Neurochem.* 57:423-430.

3. Zahniser N.R., Buck K.J., Curella P., McQuilkin S.J., Wilson-Shaw D., Miller C.L., Klein R.L., Heidenreich K.A., Keir W.J., Sikela J.M., and R.A. Harris (1992) GABA-A receptor function and regional analysis of subunit mRNAs in long-sleep and short-sleep mouse brain. *Mol. Brain Res.* 14:196-206.

4. Aguayo L.G., Pancetti F.C., Klein R.L., and R.A. Harris (1994) Differential effects of GABAergic ligands in mouse and rat hippocampal neurons. *Brain Res.* 647:97-105.

5. Klein R.L., Sanna E., McQuilkin S.J., Whiting P.J., and R.A. Harris (1994) Effects of 5-HT-3 Receptor Antagonists on Binding and Function of Mouse and Human GABA-A Receptors. *Eur. J. Pharmacol.* 268:237-246.

6. Klein R.L., Whiting P.J., and R.A. Harris (1994) Benzodiazepine treatment causes uncoupling of stably expressed GABA-A receptors. *J. Neurochem.* 63:2349-2352.

7. Mihic S.J., Whiting P.J., Klein R.L., Wafford K.A., and R.A. Harris (1995) A single amino acid of the human γ-aminobutyric acid-A receptor γ2 subunit determines benzodiazepine efficacy. *J. Biol. Chem.* 269:32768-32773.

8. Harris R.A., Proctor W.R., McQuilkin S.J., Klein R.L., Mascia M.P., Whatley V., Whiting P.J., and T. V. Dunwiddie (1995) Ethanol increases GABA-A responses in cells stably transfected with receptor subunits. *Alcohol Clin. Exp. Res.* 19:226-232.

9. Sanna E., Mascia M.P., Klein R.L., Whiting P.J., Biggio G. and R.A. Harris (1995) Actions of the general anesthetic propofol on recombinant human GABA-A receptors: influence of receptor subunits. *J. Pharmacol. Exp. Ther.* 274:353-360.

10. Klein R.L., Mascia M.P., Hadingham K.L., Harkness P.C., Whiting P.J., and R.A. Harris (1995) Regulation of allosteric coupling and function of stably transfected GABA-A receptors by GABAergic drugs. *J. Pharmacol. Exp. Ther.* 274:1484-1492.

11. Klein R.L., Mascia M.P., Whiting P.J., and R.A. Harris (1995) Binding and function of stably transfected GABA-A receptors: chronic ethanol treatments. *Alcohol Clin. Exp. Res.* 19:1338-1344.

12. Klein R.L. and R.A. Harris (1996) Regulation of GABA-A receptor structure and function by chronic drug treatments *in vivo* and with stably transfected cells. *Japanese J. Pharmacol.* 70:1-15.

13. Klein R.L., Meyer E.M., Peel A.L., Zolotukhin S., Meyers C., Muzyczka N., and M.A. King (1998) Neuron-specific transduction in the rat septohippocampal or nigrostriatal pathway by recombinant adeno-associated virus vectors. *Exp. Neurol.* 150:183-194.

14. Klein R.L., Muir D., King M.A., Peel A.L., Zolotukhin S., Möller J.C., Krüttgen A., Heymach J.V., Jr., Muzyczka N., and E.M. Meyer (1999) Long-term actions of vector-derived NGF or BDNF on choline acetyltransferase and Trk receptor levels in the adult rat basal forebrain. *Neuroscience* 90:815-821.

15. Klein R.L., McNamara R.K., King M.A., Lenox R.H., Muzyczka N., and E. M. Meyer (1999) Generation of aberrant sprouting in the adult rat brain by GAP-43 somatic gene transfer. *Brain Res.* 832:136-144.

16. Klein R.L., Lewis M.H., Muzyczka N., and E.M. Meyer (1999) Prevention of 6-hydroxydopamine-induced rotational behavior by BDNF somatic gene transfer. *Brain Res.* 847:314-320.

17. Peel A.L. and R.L. Klein (2000) Adeno-associated virus vectors: activity and applications in the central nervous system. *J. Neurosci. Methods* 98:95-104.

18. Klein R.L., Mandel R.J., and N. Muzyczka (2000) Adeno-associated virus vector-mediated gene transfer to somatic cells in the central nervous system. *Advances in Virus Res.* Vol. 55: ed. by K. Maramorosch, F.A. Murphy, A.J. Shatkin, J.C. Glorioso, Academic Press: San Diego. pp. 507-528.

19. Klein R.L., Hirko A.C., Meyers C.A., Grimes J.R., Muzyczka, N., and E.M. Meyer (2000) NGF gene transfer to intrinsic basal forebrain neurons increases cholinergic cell size and protects from age-related deficits in spatial memory in middle-aged rats. *Brain Res.* 875:144-151.

20. Andsberg G., Kokaia Z., Klein R.L., Muzyczka N., Lindvall O., and R.J. Mandel (2002) Neuropathological and behavioral consequences of adeno-associated viral vector-mediated continuous intrastriatal neurotrophin delivery in a focal ischemia model in rats. *Neurobiology of Disease* 9:187-204.

21. Klein R.L., King M.A., Hamby M.E., and E.M. Meyer (2002) Dopaminergic cell loss induced by human A30P α-synuclein gene transfer to the rat substantia nigra. *Human Gene Therapy* 13:605-612.

22. Klein R.L, Hamby M.E., Hirko A.C., Gong Y., Wang S., Hughes J.A., King M.A., and E.M. Meyer (2002) Dose and promoter effects of adeno-associated viral vector for green fluorescent protein expression in the rat brain. *Exp. Neurol.* 176:66-74.

23. Kojima M., Klein R.L., and H. Hatanaka (2002) Pre and postsynaptic modification by neurotrophins. *Neuroscience Research* 43:193-199.

24. R.L. Klein (2002) Editorial: Adeno-associated virus vectorology and gene therapy applications. *Methods* 28:145.

25. Martin R.G., Klein R.L., and H.A. Quigley (2002) Gene delivery to the eye using adeno-associated viral vectors. *Methods* 28:267-275.

26. Klein R.L., Hamby M.E., Sonntag C.F., Millard W.J., King M.A., and E.M. Meyer (2002) Measurements of vector-derived neurotrophic factor and green fluorescent protein levels in the brain. *Methods* 28:286-292.

27. King M.A., Scotty N., Klein R.L. and E.M. Meyer (2002) Particle detection, number estimation, and feature measurement in gene transfer studies: optical fractionator stereology integrated with digital image processing and analysis. *Methods* 28:293-299.

28. Larsson E., Mandel R.J., Klein R.L., Muzyczka N., Lindvall O. and Z. Kokaia (2002) Suppression of insult-induced neurogenesis in adult rat brain by brain-derived neurotrophic factor. *Exp. Neurol.* 177:1-8.

29. Li G., Klein R.L., Matheny M., King M.A., Meyer E.M. and P. J. Scarpace (2002) Induction of uncoupling protein 1 by central IL-6 gene delivery is dependent on sympathetic innervation of brown adipose tissue and underlies one mechanism of body weight reduction in rats. *Neuroscience* 115:879-889.

30. Ramirez J.J., Caldwell J.L., Majure M., Wessner D.R., Klein R.L., Meyer E.M., and M. A. King. Adeno-associated virus vector expressing nerve growth factor enhances cholinergic axonal sprouting after cortical injury in rats. *J. Neurosci.* 23:2797-2803.

31. Martin K.R.G., Quigley H.A., Zack D.J., Levkovitch-Verbin H., Kielczewski J., Valenta D., Baumrind L., Pease M.E., Klein R.L., Hauswirth W.W. Gene therapy with brain-derived neurotrophic factor protects retinal ganglion cells in a rat glaucoma model. *Invest. Opthamol. Vis. Sci.*, in press.

Exhibit B

Rapid Neurofibrillary Tangle Formation After Localized Gene Transfer of Mutated Tau

Ronald L. Klein,[1] Wen-Lang Lin,[2] Dennis W. Dickson,[2] Jada Lewis,[3] Michael Hutton,[3] Karen Duff,[4] Edwin M. Meyer,[5] Michael A. King[6, 7]

[1]Department of Pharmacology & Therapeutics, Louisiana State University Health Sciences Center, Shreveport, LA 71130. Departments of [2]Pathology and [3]Neuroscience, Mayo Clinic, Jacksonville, FL 32224. [4]Center for Dementia Research, Nathan Kline Institute, Orangeburg, NY 10962. Departments of [5]Pharmacology & Therapeutics, and [6]Neuroscience, University of Florida College of Medicine and McKnight Brain Institute, Gainesville, FL 32610, and [7]Malcom Randall Veteran's Administration Medical Center, Gainesville, FL 32610.

Correspondence should be addressed to R.L.K.(klein@lsuhsc.edu)

ABSTRACT

Neurofibrillary pathology was produced in the brains of adult rats after localized gene transfer of human tau carrying the P301L mutation, which is associated with frontotemporal dementia and parkinsonism linked to chromosome 17. Within one month of *in situ* transfection of the basal forebrain region of normal rats, tau-immunoreactive and argyrophilic neuronal lesions formed. The fibrillar lesions had features of NFTs, including argyrophilia, and tau immunoreactivity at light and electron microscopic levels. In addition to NFTs, other tau pathology, including pre-tangles and neuropil threads, was abundant and widespread. Tau gene transfer to the hippocampal region of amyloid-depositing transgenic mice produced pre-tangles and threads, as well as intensely tau-immunoreactive neurites in amyloid plaques. The ability to produce neurofibrillary pathology in adult rodents makes this a useful method to study tau-related neurodegeneration.

Tauopathies are a group of progressive neurodegenerative diseases characterized by abnormal neuronal and often glial accumulations of the microtubule-associated protein tau (1, 2). In the adult nervous system tau is preferentially localized to axons (3), where it contributes to dynamic properties of microtubules, including fast axonal transport of vesicular structures (4). In human tauopathies tau is phosphorylated excessively and on amino acid residues not usually modified (5-7), resulting in abnormal conformations (8) that are likely to interfere with a variety of intracellular functions (9-12) and even cellular survival (6). The selective axonal compartmentation of tau is also lost as abnormal tau accumulates in neuronal perikarya and dendrites (13). In many familial and sporadic tauopathies tau is detected in glial cells as well (14). Intracellular lesions develop as non-fibrillar aggregates referred to as "pre-tangles" (15). Over time these progress into argyrophilic, filamentous neurofibrillary tangles (NFTs). At the electron microscopic level, pathologic tau filaments take a variety of forms, including paired helical filaments and straight filaments, which are relatively disease-specific and related to the tau isoform composition of fibrils (2). In Alzheimer's disease (AD), NFTs composed of 3R and 4R tau (isoforms containing 3 or 4 repeats of a 31-32 residue motif in the microtubule-binding domain) usually appear as paired helical filaments. In the most common tauopathies, which are associated with preferential accumulation of 4R tau, the filaments are straight or twisted ribbons (5).

NFTs characterize the neurodegeneration found in the tauopathies, but they are also a diagnostic necessity for (AD; 16), and their density and distribution correlate with cognitive deficits even in early stages (17, 18). NFTs have been difficult to study experimentally because they rarely develop in subprimates (19). As a result it is not fully understood how pre-tangles and NFTs are linked to neurodegeneration or to senile plaques that are the other major histopathologic lesion in AD. With the discovery of mutations in the tau gene it has become possible to employ mutant tau in experimental analyses of neurofibrillary pathology. Current animal models of transgenic tau expression in flies (20), zebrafish (21), lampreys (22), and mice (23-27) have

provided a wealth of information about tau pathology. In particular, the P301L mutation, which is the most common cause of frontotemporal dementia and parkinsonism linked to chromosome 17 (FTDP-17; 1), has been used in developing mouse models that share structural and biochemical features with human tauopathies (23-25).

Somatic cell gene transfer can complement and extend the whole animal transgenic approach for analyzing the neurobiological function of gene products. Brain regions can be selectively targeted and regions not transfected can serve as within-animal controls. The onset of expression of target genes can be controlled to bypass potential developmental effects and study the temporal course of pathophysiology or adaptation to mutant gene expression. The effects of multiple transgenes can be studied without the need to develop new breeding lines. Along this line, both lentivirus and adeno-associated virus (AAV) vector-based systems have led to nigrostriatal degeneration models in rats via alpha-synuclein gene transfer (28, 29). We used AAV vector-based somatic gene transfer to produce localized expression of mutant tau to generate neurofibrillary pathology. In addition to using this in normal animals we also transferred mutant tau to transgenic mice which develop robust amyloid plaque pathology at an early age as a consequence of expressing mutant forms of presenilin and amyloid precursor protein (PS1/APP mice; 30).

RESULTS

DNA for P301L mutant tau (4R2N; 30) was incorporated into two AAV-2 expression plasmids (31). The pTau-W construct contained the hybrid chicken beta actin/cytomegalovirus (CBA) promoter (32) and the WPRE (woodchuck hepatitis virus post-transcriptional regulatory element; 33), and a second construct, pCB-Tau, contained only the CBA promoter. Protein extracts of cells transduced with either vector produced a major band at about 70 kDa on western blots for human-specific tau (T-14; Fig. 1), and the WPRE construct appeared to produce more tau expression under the same experimental conditions (lanes 1 & 2). Both P301L

4R2N tau AAV vectors were evaluated in rat whole brain primary neuron cultures (34) and in the rat brain. Tau expression was detected in primary neuronal cultures after 5 days with the pTau-W AAV vector, but no expression was detected from similar treatments with pCB-Tau AAV (Fig. 1, lanes 3-7). The WPRE therefore boosted tau expression in neuronal cultures as previously reported for green fluorescent protein (GFP; 31). Tau transgene expression was detected on western blots after injections of the vectors into the medial septal region of the basal forebrain of 3 month old male Sprague-Dawley rats (38). Immunoblots for total human tau (T-14; Fig. 1, lanes 8, 9) or hyperphosphorylated tau (CP13; Fig. 1, lanes 10, 11) demonstrated expression *in vivo* for both constructs.

The control AAV vector containing a GFP gene led to robust expression in the rat basal forebrain (Fig. 2A and 2B). Within 3 weeks of injection of tau vectors, many neurons around the injection path contained human tau identified by immunofluorescent or immunoperoxidase labeling. Neurons, but not glia, were immunoreactive and labeling was present in perikarya, dendrites and neuritic arbors as described for AD (13, 35).

The expression was localized to the medial septum (1-1.5 mm anterior and posterior from the injection site) ipsilateral to the injection (Fig. 2C). Tau-immunoreactive axons were detected throughout the ipsilateral fimbria, fornix and hippocampus. The human-specific tau antibody T-14 did not label any structures in rat brain tissue after sham injections or transduction with control vector. Tau expression persisted for at least 8 months after injections, the longest interval tested in rats. Tau immunoreactivity was dense in neuronal perikarya, and the cells had distorted cytologic features that differed from normal pyramidal neurons (Fig. 2D), resembling flame-shaped NFTs. Immunolabeling for several antibodies against hyperphosphorylated tau and disease-related conformational tau epitopes (8) was tested. The monoclonal antibody CP13 recognizes phosphorylated tau serine 202. CP13 labeled diffuse or finely granular perikaryal cytoplasmic neuronal immunoreactivity from one month to eight months, the longest interval tested (Fig. 2E). The distribution of

CP13-immunoreactivity was similar to that found with the human-specific antibody T-14, demonstrating that the human tau was hyperphosphorylated within the earliest interval tested, 3 weeks. Antibodies to other pathological epitopes described in NFTs confirmed similar neuronal pathology in rats to that seen in human disease. The monoclonal tau antibody AT100, which specifically recognizes relatively AD-specific phosphorylated serine residues (Ser212 and Ser214), showed a different pattern than CP13, appearing mainly in varicose neurites near the injection sites rather than in neuronal cell bodies. Staining with AT100 was less widespread than with CP13. The Alz-50 antibody, which recognizes an abnormal tau conformation found in AD (36), gave similar results as AT100 with the pCB-Tau AAV vector. With the pTau-W AAV vector, the neurofibrillary pathology reflected by Alz-50 staining (Fig. 3A) appeared more intense and over larger tissue volumes than after comparable injections of pCB-tau AAV (not shown). It appeared that a larger fraction of the total human tau T-14 immunoreactivity was also positive for Alz-50 in the case of the WPRE vector. The pTau-W vector expressed immunoreactivity for the NFT-specific antibody Ab-39 (37) in cell bodies and processes throughout the medial septum (Fig. 3B). Gallyas silver staining, which labels fibrillary argyrophilic lesions, revealed NFTs and neuritic processes 3 weeks after injection of the pCB-Tau AAV (Fig. 3C). Argyrophilia was examined on sections adjacent to those used for CP13 immunolabeling (Fig. 3D & E). Only some of the CP13-immunoreactive cells, i.e. those with globose immunoreactivity, demonstrated silver staining.

Samples processed for transmission electron microscopy (EM) showed neuronal cell bodies and cell processes containing 15-20 nm diameter straight filaments (not shown), consistent with P301L tau filaments detected in NFTs in transgenic mice (23, 25). ImmunoEM demonstrated unequivocally that these filamentous lesions contained tau. ImmunoEM with CP13 showed immunolabeling of 15-20 nm diameter straight filaments (Fig. 3F). Similar ultrastructural results were also obtained with a polyclonal antibody specific to human tau (E-1; 38) and with a monoclonal antibody (MC-1; 36) specific to a pathologic conformation found

in tau in AD (8). Tau immunoreactivity was detected at the electron microscopic level at 2 months, but the number of gold particles was sparse. There were no pathologic filaments or identifiable NFTs at 2 months. Some neurons also showed pre-tangle-like staining patterns at 4 months as was found at earlier intervals.

We injected vectors into the hippocampi of 2-month-old doubly transgenic PS1/APP mice (30), attempting to add neurofibrillary pathology to an existing transgenic background that has become an important model for AD. The GFP control vector produced efficient transfection of pyramidal and non-pyramidal neurons in CA1 and dentate gyrus that lasted at least 12 months (Fig. 4A). After delivery of pCB-tau AAV, similarly persistent expression in ipsilateral dentate granule neurons was demonstrated by immunoreactivity for the human-specific tau T-14 antibody (Fig. 4B). Immunolabeling with a panel of tau antibodies revealed that the pCB-Tau AAV vector produced neuronal tau pathology in the mouse hippocampus similar to that observed with injections into the septal region of rats. Both thioflavine S fluorescence and immunofluorescence for amyloid, demonstrated with a monoclonal antibody to an amino-terminal epitope in Aβ (6E10), showed amyloid deposits throughout the hippocampus and cortex. Some neurons with tau-immunoreactive pre-tangles were found in close proximity to amyloid deposits (Fig. 4C). The amyloid plaques were also frequently penetrated and surrounded by tau-immunoreactive neurites (Fig. 4D), reminiscent of neuritic dystrophy associated with plaques in AD (39).

DISCUSSION

Human mutant P301L tau was expressed in the brains of adult rats and mice with somatic cell gene transfer. The rat is a versatile animal model for many pharmacological and behavioral probes. The expression of NFTs, perhaps the most common neuropathological lesions found across the broadest range of neurodegenerative diseases, in this species will facilitate studies of factors that influence NFT formation. For example, the influence of the aged brain can be evaluated by comparing results from vector injections at the

same dose and time interval, in either young or old subjects. Such an experiment would be difficult in existing models of tauopathy, but addressable with a vector approach because the onset of transgenic expression can be controlled. Another advantage of this approach is the ability to combine transgenes, which we demonstrated by expressing at least pre-tangle tau pathology in the brains of amyloid mice. We found tau-immunoreactive neurites closely associated with amyloid plaques. This approach may therefore provide a novel experimental method to model AD pathology comprehensively, in which relationships between amyloid and tau *in vivo* can be analyzed systematically.

The degree of tau pathology appeared to be expression level- and time-dependent. The combination of the CBA promoter and the WPRE in AAV serotype 2 vectors boosted expression levels of GFP in neurons to significantly higher levels than in similar vectors without the WPRE (31). The same was true for tau vectors, with the CBA-tau-WPRE AAV producing detectable tau expression in primary neuronal cultures, while the CBA-tau AAV did not. The greater expression of tau conferred by the WPRE also led to greater pathology, as a more complete fraction of the total tau immunoreactivity was also positive for Alz-50 immunoreactivity in the case of the CBA-tau-WPRE vector. Expressing more tau within neurons led to more AD-like Alz50 tau conformations. NFTs were unequivocally detected by immunoEM at 4 months but not at 2 months, suggesting that NFT formation was time-dependent over this interval in this model. The sparse pre-tangle-like deposition of gold particles observed at 2 months was also found in some neurons at 4 months, which may suggest that NFT formation is not complete by 4 months. The fact that positive Gallyas staining could be found in a few cells within 3 weeks suggests that NFT formation may be occurring much faster in cells that are expressing the highest levels of tau or that some cells are more prone to be tangle-genic, potentially due to differential expression of kinases that may phosphorylate tau.

The vector approach can be used to successfully model NFTs in adult rats. This model will be useful for studying the pathogenesis of neurodegeneration. The ability to target specific neuronal populations

affected in human disease makes it possible to generate animal models that are more complete approximations of specific diseases, which may facilitate the development of rational therapeutic interventions.

METHODS

DNAs, transfections, western blots

DNAs to be expressed were incorporated into expression cassettes that are flanked by the AAV serotype 2 terminal repeats, the only remaining sequence (and 4%) of the AAV-2 genome. The CBA promoter was used for all constructs and in some cases the 3' enhancer WPRE. Control GFP plasmids were described previously (29, 31). Constructs were made several forms of tau including wild type and P301L forms either with or without exons 2/3 (23, 25). Plasmids were carried in SURE *E.coli* (Strategene) and CsCl-purified.

Immunoblots were run with samples from transfected human embryonic kidney 293 cells. The calcium-phosphate method was used for transfection, with 2 $x10^6$ cells on 6 cm dishes and 8 μg of DNA per dish. Two days after transfection, 293 cells were scraped into 0.5 ml cold homogenization buffer (1% Nonidet P-40, 0.5 % sodium deoxycholate, 0.1% SDS in 1X PBS, also containing protease inhibitors: 0.1 mg/ml PMSF, 1 μg/ml aprotinin, 1 mM sodium orthovanadate), sonicated for 5 sec, spun at top speed in a microcentrifuge for 5 min, and the supernatant was used for western blots. Each of the DNA constructs was transfected in 293 cells and produced the appropriate sized bands on human tau-specific T-14 immunoblots (60 kDa for 2/3- forms and 70 kDa for 2/3+ forms), which were not found in controls. Only the P301L form including exons 2/3 was packaged into AAV and expressed in primary neuronal cultures and in the rat brain.

Primary neuronal cultures were provided by the laboratory of Dr. Colin Sumners at the University of Florida. The preparations were from whole brains of newborn Sprague-Dawley rats as previously described (34, 31). The cultures contained $3x10^6$ cells per well of 6-well dishes. Ten days after plating, the AAV was

added, in volumes between 1-30 µl. Cells were harvested 5 days later for tau immunoblots as described above.

For the brain tissue, a 3 mm coronal section of the forebrain was taken using a 1 mm brain block device. The medial septum/vertical limb of diagonal band on the side of the injection was dissected. The sample was weighed and homogenized in 0.5 ml of the same buffer as above using a small Dounce homogenizer, spun as above, and the supernatant was collected. All samples were normalized for protein content by Bradford assay and subjected to 12% SDS/polyacrylamide gel electrophoresis.

Vector packaging and titering

Packaging of plasmids in recombinant AAV serotype 2 was based on the streamlined method developed by Zolotukhin *et al.* (40), and described by Klein *et al.* (29). Briefly, 293 cells were transfected with an AAV terminal repeat-containing plasmid in an equimolar ratio with the plasmid pDG, which provides the AAV coat protein genes, and adenovirus 5 genes necessary for helper function in packaging (41). Three days after transfection, cells and media were harvested and pelleted. The pellet was resuspended in lysis buffer (50 mM Tris pH 8.5, 150 mM NaCl) and freeze-thawed 3 times. The sample was then incubated with 1500 units of endonuclease (Sigma) for 30 min. at 37°C. After, the sample was centrifuged at 3700 RPM and the resulting supernatant was applied to a discontinuous gradient of iodixinol (OptiPrep, Nycomed). The AAV was then removed and added to a heparin (Sigma) affinity column and the eluent was concentrated and washed using Millipore Biomax 100 Ultrafree-15 units. AAV vector stocks were titered for physical particles, or copies of vector genomes, by dot-blotting against standard curves of known amounts of DNA using the non-radioactive BrightStar kit (Ambion). Titers for the AAVs that were used were between 1×10^{12} and 1×10^{13} particles per ml.

Subjects and stereotaxic injections

Male Sprague-Dawley rats (3 months old) were anesthetized with a cocktail of 3 ml xylazine (20 mg/ml), 3 ml ketamine (100 mg/ml), and 1 ml acepromazine (10 mg/ml) administered intramuscularly at a dose of 0.5-0.7 ml/kg. The injection coordinates for the medial septum were 0.7 mm bregma, 0.2 mm lateral, 7.0 mm ventral (42). Virus stocks were injected through a 27 ga. cannula connected via 26 ga. I.D. polyethylene tubing to a 10 µl Hamilton syringe mounted to a CMA/100 microinjection pump. The pump delivered 3 µl at a rate of 0.2 µl/min, and the needle remained in place at the injection site for 1 additional min. The cannula was removed slowly (over 2 min), and the skin was sutured and the animal was placed on a heating pad until it began to recover from the surgery, before being returned to their individual cages. Two month old double transgenic PS1/APP mice (30) were injected with AAV vectors in the hippocampus, -2.1 mm bregma, 1.2 mm lateral, 2.0 mm ventral (43). The anesthetic for mice was isoflurane using a gas anesthesia system. Two µl of AAV vector was injected with a 30 ga. needle. All animal care and procedures were in accordance with institutional IACUC and NIH guidelines.

Histological staining for light and electron microscopy

Anesthetized animals were perfused with cold phosphate-buffered saline (PBS), followed by cold 4% paraformaldehyde in PBS. The brain was removed and immersed in fixative overnight at 4°C. For standard immunohistochemistry, the brain was equilibrated in a cryoprotectant solution of 30% sucrose/PBS at 4°C. Coronal sections (50 µm thick) were cut on a sliding microtome with freezing stage. Antigen detection was conducted on free-floating sections by incubation in a blocking solution (2% goat serum/0.3% Triton X-100/ PBS) for 1 hr at room temperature, followed by primary antibody incubation overnight at 4°C on a shaking platform. Prior to blocking, endogenous peroxidase was quenched by incubation in 0.5% H_2O_2/PBS for 10 min. The sections were washed in PBS, and incubated with biotinylated goat anti-rabbit or goat anti-mouse

secondary antibody (DAKO, 1:1000) for 1 hr at room temperature. The sections were washed with PBS and labeled with horseradish peroxidase (HRP)-conjugated Extravidin (Sigma, 1:1000) for 30 min at room temperature. Development of tissue labeled with HRP was conducted with a solution of 0.67 mg diaminobenzidine (Sigma), 0.13 µl of 30% H_2O_2 per ml of 80 mM sodium acetate buffer containing 8 mM imidazole and 2% $NiSO_4$. Peroxidase-stained sections were mounted on Fisher Superfrost Plus glass slides, dehydrated in a series of ethanol and xylene incubations and coverslipped with Eukitt (Electron Microscopy Sciences). Primary antibodies for immunostaining included: GFP (Molecular Probes, 1:2000); Tau T-14 (Zymed, 1:2000); anti-NFT (Chemicon, 1:200); CP13 (P. Davies, Albert Einstein College of Medicine, 1:200); Alz-50 (P. Davies, 1:200); MC-1 (S.H. Yen, Mayo Clinic Jacksonville, 1:500); E-1 (S.H. Yen, 1:500), Ab-39 (S.H. Yen, 1:500); AT100 (1:500, Endogen); 6E10 (1:1000, Serotec). Some of the markers were visualized with immunofluorescence using TRITC-conjugated or coumarin-conjugated secondary antibodies (1:500, Jackson ImmunoResearch). Flourescent samples were coverslipped with glycerol-gelatin (Sigma).

For Gallyas silver staining and immunoEM, the animals were perfusion fixed and the brains were extracted and immersed in fixative overnight as above. The brains were then placed in PBS. Tissue blocks of the medial septum/vertical limb of diagonal band were paraffin embedded for Gallyas or plastic embedded for immunoEM as described (23, 25). Gallyas samples were counterstained for hematoxylin & eosin. For regular EM, animals were perfused with normal saline and then 2.5% glutaraldehyde/ 2% formaldehyde in 0.1 M sodium cacodylate buffer. The brains were immersed in fixative overnight and then placed in 0.1 M sodium cacodylate before processing for plastic embedding (23, 25).

Acknowledgements

We thank Dr. P. Davies (Albert Einstein College of Medicine) for antibodies CP13, Alz-50, and MC-1 and Dr. S.H. Yen (Mayo Clinic Jacksonville) for antibodies E-1 and Ab-39, and acknowledge the technical

contributions of Craig Meyers and Aaron Hirko. Supported by NIA AG10485.

REFERENCES

1. Hutton, M. *et al.* Association of missense and 5'-splice-site mutations in tau with the inherited dementia FTDP-17. *Nature.* **393**:702-5 (1998).

2. Spillantini, M.G., Bird, T.D., & Ghetti, B. Frontotemporal dementia and Parkinsonism linked to chromosome 17: a new group of tauopathies. *Brain Pathol.* **8**:387-402 (1998).

3. Binder L.I., Frankfurter, A., & Rebhun, L.I. The distribution of tau in the mammalian central nervous system. *J Cell Biol.* **101**:1371-8. (1984)

4. Stamer, K., Vogel, R., Thies, E., Mandelkow, E., & Mandelkow, E.M. Tau blocks traffic of organelles, neurofilaments, and APP vesicles in neurons and enhances oxidative stress. *J Cell Biol.* **156**:1051-63. (2002)

5. Buee, L., Bussiere, T., Buee-Scherrer, V., & Delacourte, A. Tau protein isoforms, phosphorylation and role in neurodegenerative disorders. *Brain Res Brain Res Rev.* **33**:95-130 (2000).

6. Kobayashi, K., *et al.* Association of phosphorylation site of tau protein with neuronal apoptosis in Alzheimer's disease. *J Neurol Sci.* **208**:17-24 (2003).

7. Liu, F., Iqbal, K., Grundke-Iqbal, I., Gong, C.X. Involvement of aberrant glycosylation in phosphorylation of tau by cdk5 and GSK-3beta. *FEBS Lett.* **530**:209-14 (2002).

8. Weaver, C.L., Espinoza, M., Kress, Y., & Davies, P. Conformational change as one of the earliest alterations of tau in Alzheimer's disease. *Neurobiol Aging.* **21**:719-27 (2000).

9. Selden, S.C. & Pollard, T.D. Phosphorylation of microtubule-associated proteins regulates their interaction with actin filaments. *J Biol Chem.* **258**:7064-71 (1983).

10. Keck, S., Nitsch, R., Grune, T., & Ullrich, O. Proteasome inhibition by paired helical filament-tau in brains of patients with Alzheimer's disease. *J Neurochem.* **85**:115-22 (2003).

11. Alonso, A.C., Grundke-Iqbal, I., & Iqbal, K. Alzheimer's disease hyperphosphorylated tau sequesters normal tau into tangles of filaments and disassembles microtubules. *Nat Med.* **2**:783-7 (1996).

12. Arawaka, S. *et al.* The tau mutation (val337met) disrupts cytoskeletal networks of microtubules. *Neuroreport.* 1999 **10**:993-7 (1999).

13. Kowall, N.W. & Kosik, K.S. Axonal disruption and aberrant localization of tau protein characterize the neuropil pathology of Alzheimer's disease. *Ann Neurol.* **22**:639-43 (1987).

14. Chin, S.S. & Goldman, J.E. Glial inclusions in CNS degenerative diseases. *J Neuropathol Exp Neurol.* **55**:499-508 (1996).

15. Bancher, C. *et al.* Accumulation of abnormally phosphorylated tau precedes the formation of neurofibrillary tangles in Alzheimer's disease. *Brain Res.* **477**:90-9 (1989).

16. Hyman, B.T. & Trojanowski J.Q. Consensus recommendations for the postmortem diagnosis of Alzheimer disease from the National Institute on Aging and the Reagan Institute Working Group on diagnostic criteria for the neuropathological assessment of Alzheimer disease. *J Neuropathol Exp Neurol.* **56**:1095-7 (1997).

17. Grober, E. *et al.* Memory and mental status correlates of modified Braak staging. *Neurobiol Aging.* **20**:573-9 (1999).

18. Riley, K.P., Snowdon, D.A., & Markesbery, W.R. Alzheimer's neurofibrillary pathology and the spectrum of cognitive function: findings from the Nun Study. *Ann Neurol.* **51**:567-77 (2002).

19. van Slegtenhorst, M., Lewis, J., & Hutton, M. The molecular genetics of the tauopathies. *Exp Gerontol.* **35**:461-71 (2000).

20. Wittmann, C.W. *et al.* Tauopathy in Drosophila: neurodegeneration without neurofibrillary tangles. *Science.* **293**:711-4 (2001).

21. Tomasiewicz, H.G., Flaherty, D.B., Soria, J.P., & Wood, J.G. Transgenic zebrafish model of neurodegeneration. *J Neurosci Res.* **70**:734-45 (2002).

22. Hall, G.F., Yao, J., & Lee, G. Human tau becomes phosphorylated and forms filamentous deposits when overexpressed in lamprey central neurons in situ. *Proc Natl Acad Sci U S A.* **94**:4733-8 (1997).

23. Lewis, J. & *et al.* Neurofibrillary tangles, amyotrophy and progressive motor disturbance in mice expressing mutant (P301L) tau protein. *Nat Genet.* **25**:402-5 (2000).

24. Götz, J., Chen, F., Barmettler, R., & Nitsch, R.M. Tau filament formation in transgenic mice expression P301L tau. *J Biol. Chem.* **5**:529-534 (2001).

25. Lin, W.L., Lewis, J., Yen, S.H., Hutton, M., & Dickson, D.W. Filamentous tau in oligodendrocytes and astrocytes of transgenic mice expressing the human tau isoform with the P301L mutation. *Am J Pathol.* **162**:213-8 (2003).

26. Tanemura, K. *et al.* Neurodegeneration with tau accumulation in a transgenic mouse expressing V337M human tau. *J Neurosci.* **22**:133-41 (2002).

27. Allen, B. *et al.* Abundant tau filaments and nonapoptotic neurodegeneration in transgenic mice expressing human P301S tau protein. *J Neurosci.* **22**:9340-51 (2002).

28. Lo Bianco, C. *et al.* Alpha -Synucleinopathy and selective dopaminergic neuron loss in a rat lentiviral-based model of Parkinson's disease. *Proc Natl Acad Sci U S A.* **99**:10813-8 (2002).

29. Klein, R.L., King, M.A., Hamby, M.E., & Meyer, E.M. Dopaminergic cell loss induced by human A30P alpha-synuclein gene transfer to the rat substantia nigra. *Hum Gene Ther.* **13**:605-12 (2002).

30. Holcomb, L. *et al.* Accelerated Alzheimer-type phenotype in transgenic mice carrying both mutant amyloid precursor protein and presenilin 1 transgenes. *Nat Med.* **4**:97-100 (1998).

31. Klein, R.L. *et al.*, Dose and promoter effects of adeno-associated viral vector for GFP expression in the rat brain. *Exp. Neurol.* **176**, 66 (2002).

32. Niwa, H., Yamamura, K., & Miyazaki, J. (1991) Efficient selection for high-expression transfectants with a novel eukaryotic vector. *Gene* **108**:193-9.

33. Loeb, J.E., Cordier, W.S., Harris, M.E., Weitzman, M.D., & Hope, T.J. Enhanced expression of transgenes from adeno-associated virus vectors with the woodchuck hepatitis virus posttranscriptional regulatory element: implications for gene therapy. *Hum Gene Ther.* **10**:2295-305 (1999).

34. Chou, Y.C., Luttge, W.G., & Sumners, C. Characterization of glucocorticoid type II receptors in neuronal and glial cultures from rat brain. *J. Neuroendocrinol.* **2**, 29-38 (1990).

35. Braak, E., Braak, H., & Mandelkow, E.M. A sequence of cytoskeleton changes related to the formation of neurofibrillary tangles and neuropil threads. *Acta Neuropathol (Berl).* **87**:554-67 (1994).

36. Jicha, G.A., Bowser, R., Kazam, I.G., & Davies, P. Alz-50 and MC-1, a new monoclonal antibody raised to paired helical filaments, recognize conformational epitopes on recombinant tau. *J Neurosci Res.* **48**:128-32 (1997).

37. Dickson, D.W. *et al.,* Diffuse Lewy body disease: light and electron microscopic immunocytochemistry of senile plaques *Acta Neuropathol.* **78**, 572 (1989).

38. Crowe,A., Ksiezak-Reding, H., Liu, W.K., Dickson, D.W. & Yen, S.H. The N terminal region of human tau is present in Alzheimer's disease protein A68 and is incorporated into paired helical filaments. *Am J Pathol,* **139**, 1463-70 (1991)

39. Dickson, D.W. The pathogenesis of senile plaques. *J. Neuropathol. Exp. Neurol.* **56**, 321 (1997).

40. Zolotukhin, S. *et al.*, Recombinant adeno-associated virus purification using novel methods improves infectious titer and yield. *Gene Therapy.* **6**:973-985 (1999).

41. Grimm, D., Kern, A., Rittner, K., & Kleinschmidt, J.A. Novel tools for production and purification of recombinant adeno-associated virus vectors. *Hum Gene Ther.* **9**:2745-2760 (1998).

42. Paxinos, G. & Watson, C. The rat brain in stereotaxic coordinates. Academic Press, San Diego (1998).

43. Paxinos, G. & Franklin, K.B.J. The mouse brain in stereotaxic coordinates. Academic Press, San Diego (2001).

Figure Legends

Fig. 1. Tau AAV vector expression *in vitro* and *in vivo*. The form of tau was the human P301L including exons 2 & 3, and the main protein band produced ran at approximately 70 kDa, as expected. Lanes 1 & 2, Tau T-14 immunoblot, 20 μg of either the pCB-Tau (lane 1) or the pTau-W (lane 2) DNAs were transfected into HEK 293 cells, 20 μg protein per lane. Lanes 3-7 Tau T-14 immunoblot, $4x10^{10}$ particles of either the pCB-Tau AAV (lanes 3 & 4) or the pTau-W AAV (lanes 5 & 6) was added to day 10 neonatal rat whole brain neuronal cultures. After 5 days, the 70 kDa band was detected only in cultures that were treated with the WPRE-containing vector. Lane 7, untreated primary neuron culture sample, all samples had a similar band around 65 kDa, 20 μg protein in lanes 3-7. Lanes 8 & 9, Tau T-14 immunoblot, dissected and homogenized basal forebrain after injection of $1x10^{10}$ particles of the pCB-Tau AAV (lane 8, 6 months post-injection) or $1x10^{10}$ particles of the the pTau-W AAV (lane 9, 1 month post-injection), 70 μg protein per lane. Lanes 10 & 11, hyperphosphorylated tau antibody CP13 immunoblot, pCB-Tau and pTau-W as in lanes 8 & 9.

Fig. 2. GFP and tau expression in the rat basal forebrain. A) The medial septal nucleus/diagonal band was injected, leading to widespread expression of GFP immunoreactivity throughout this area. Serial sections from 1 brain injected with the control pGFP AAV (31), $1x10^{10}$ particles in 3 μl, 2 months post-injection. B) Native GFP fluorescence after the unilateral injections as in A, which is not as sensitive in detecting GFP expression as the immunostaining in A. C) Human-specific Tau T-14 staining 3 weeks after injecting the pCB-Tau AAV ($1x10^{10}$ particles in 3 μl) showing widespread expression of the human tau in the same area as A & B. D) The cells expressing T-14 immunoreactivity had sharp pointed edges, not unlike in appearance to flame-shaped NFTs. Inset, higher magnification E) CP13 hyperphosphorylated tau immunoreactivity, 2 months post-injection pTau-W AAV ($1x10^{10}$ particles; immunofluorescence). The expression pattern for CP13 was similar to that of total tau T-14 immunoreactivity at all intervals tested and with both tau vectors.

Bars, A = 4.2 mm; B, C = 200 μm; D = 25 μm; E = 40 μm.

Fig. 3. Neurofibrillary pathology and NFT formation in the rat brain. A) Alz-50 staining after injection of the WPRE-containing Tau vector, $1x10^{10}$ particles, 1 month post-injection. The Alz-50 staining was more pronounced than with the pCB-Tau AAV (not shown), although this conformational epitope was still mainly expressed in fine neurites. B) The NFT-specific antibody Ab-39 labeled dystrophic cells and neurites along the needle track at 4 months, pTau-W AAV. C) Gallyas silver staining was detected in neuron cell bodies and processes at 3 weeks post-injection, pCB-Tau AAV, $1x10^{10}$ particles. D & E) Labeling on adjacent sections with CP13 and Gallyas staining showed that a small fraction of CP13-positive cells were argyrophilic. The globose staining for CP13 (arrow in H) was also positive for Gallyas (arrow in I), a confirmed NFT at 4 months, pTau-W AAV. F) ImmunoEM was performed using the CP13 antibody. At 4 months, gold particles labeled along 15-20 nm filaments, which were found aggregated into bundles, pTau-W AAV. Inset, 3-fold higher magnification. Similar results were found with the conformational MC-1 antibody and the human-specific E-1 antibody. Bar, A, B, D, E = 15 μm; C = 10 μm; F = 300 nm.

Fig. 4. GFP and tau expression in amyloid-bearing mice. A) The GFP control vector, pTR-UF12 (29, 31), was efficient for expression in CA1 and dentate gyrus granule cells after hippocampal injections to PS1/APP double transgenic mice, $6x10^9$ particles in 2 μl injected, 12 months post-injection, DAPI counterstain, midline to right. The DAPI-dense loci proved to be amyloid plaques on adjacent sections stained with the 6E10 antibody. B) Tau T-14 immunofluorescence (red) in cell bodies and processes in the dentate gyrus, midline to left, $6x10^9$ particles of pCB-Tau AAV injected, 12 months post-injection. The T-14-stained neurites appeared to be enriched around loci the size of plaques. The green fibers are commissural axons of neurons transduced by GFP control vector injected on the contralateral side as in A. C) Anti-NFT antibody-staining (red) and 6E10-staining (blue) after injections as in B. D) Plaques near the pCB-Tau AAV injections were surrounded

by rings of anti-NFT staining as in C. Bars, A, B, D = 50 μm; C = 100 μm.

Fig. 1.

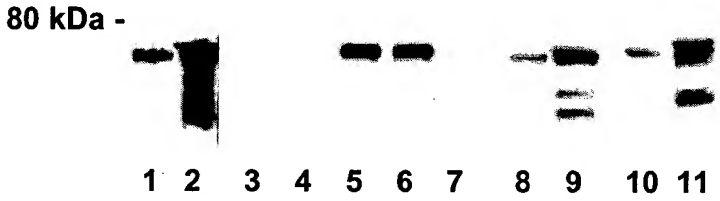

Fig. 2.

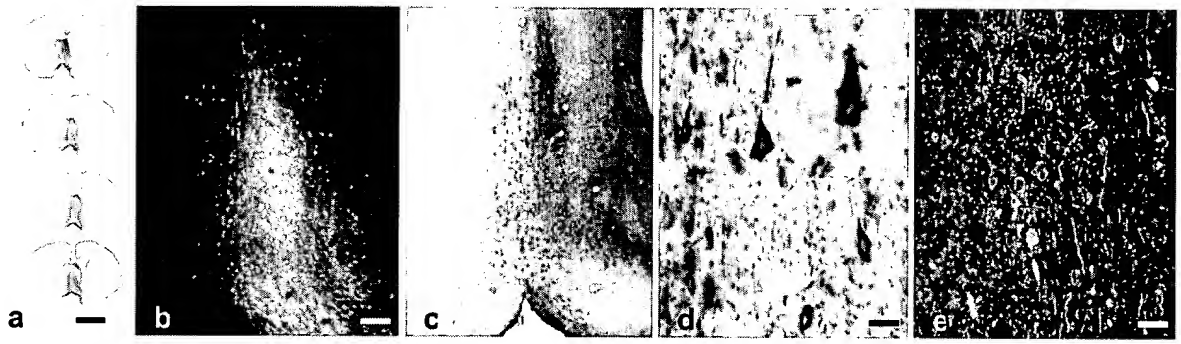

Fig. 3.

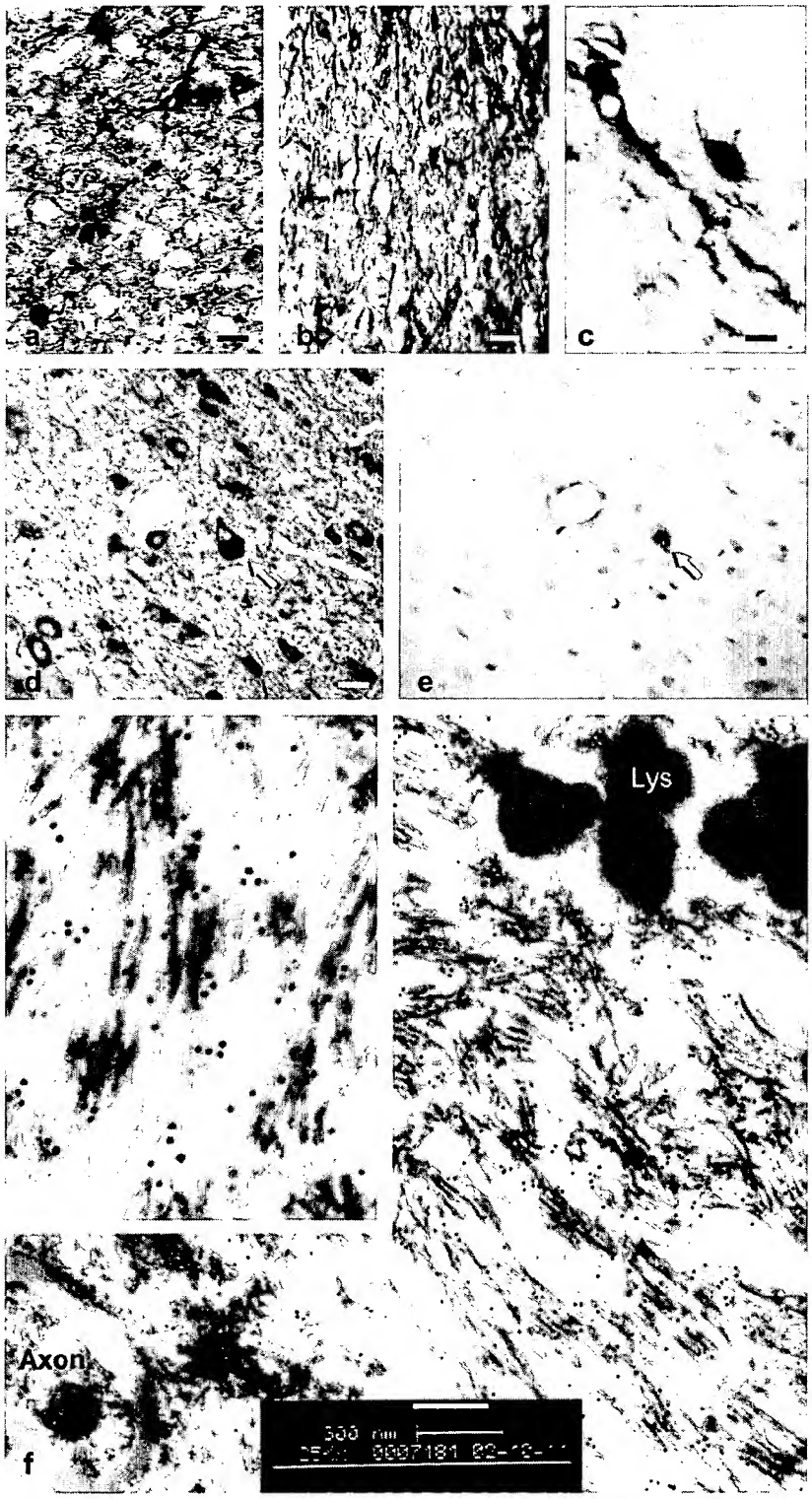

Fig. 4.

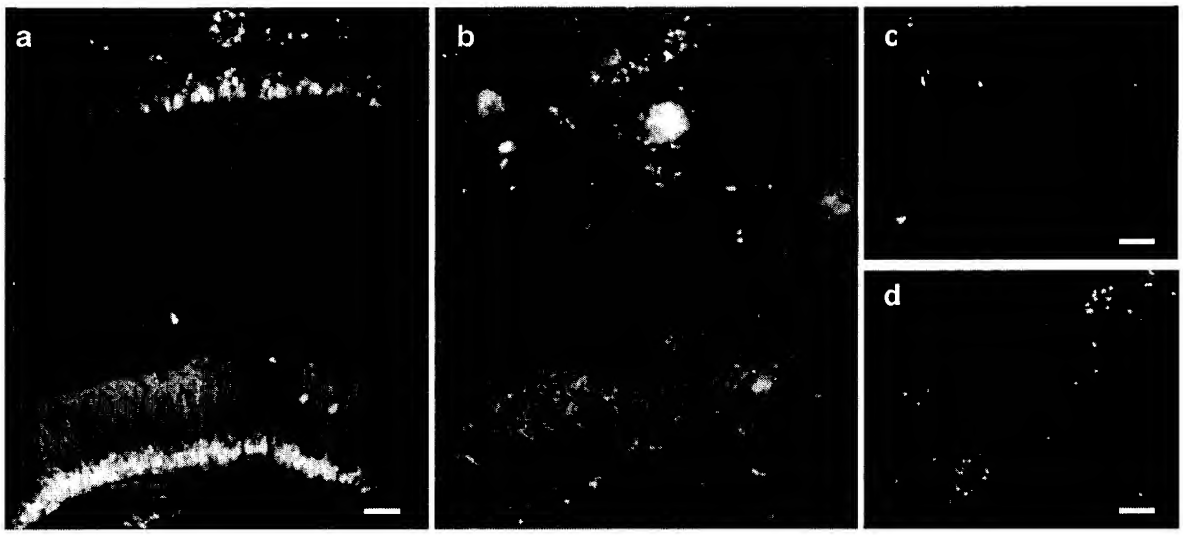

Exhibit C

Nigrostriatal α-synucleinopathy induced by viral vector-mediated overexpression of human α-synuclein: A new primate model of Parkinson's disease

Deniz Kirik*†, Lucy E. Annett‡, Corinna Burger§¶, Nicholas Muzyczka§¶, Ronald J. Mandel¶‖, and Anders Björklund*

*Wallenberg Neuroscience Center, Department of Physiological Sciences, Division of Neurobiology, Lund University, BMC A11, 221 84 Lund, Sweden; ‡Psychology Department, University of Hertfordshire, College Lane, Hatfield, Hertfordshire AL10 9AB, United Kingdom; and §Department of Molecular Genetics and Microbiology, and ‖Department of Neuroscience, McKnight Brain Institute, and ¶Powell Gene Therapy Center, University of Florida, P.O. Box 100244, Gainesville, FL 32610

Edited by Ann M. Graybiel, Massachusetts Institute of Technology, Cambridge, MA, and approved January 7, 2003 (received for review October 21, 2002)

We used a high-titer recombinant adeno-associated virus (rAAV) vector to express WT or mutant human α-synuclein in the substantia nigra of adult marmosets. The α-synuclein protein was expressed in 90–95% of all nigral dopamine neurons and distributed by anterograde transport throughout their axonal and dendritic projections. The transduced neurons developed severe neuronal pathology, including α-synuclein-positive cytoplasmic inclusions and granular deposits; swollen, dystrophic, and fragmented neuritis; and shrunken and pyknotic, densely α-synuclein-positive perikarya. By 16 wk posttransduction, 30–60% of the tyrosine hydroxylase-positive neurons were lost, and the tyrosine hydroxylase-positive innervation of the caudate nucleus and putamen was reduced to a similar extent. The rAAV-α-synuclein-treated monkeys developed a type of motor impairment, i.e., head position bias, compatible with this magnitude of nigrostriatal damage. rAAV vector-mediated α-synuclein gene transfer provides a transgenic primate model of nigrostriatal α-synucleinopathy that is of particular interest because it develops slowly over time, like human Parkinson's disease (PD), and expresses neuropathological features (α-synuclein-positive inclusions and dystrophic neurites, in particular) that are similar to those seen in idiopathic PD. This model offers new opportunities for the study of pathogenetic mechanisms and exploration of new therapeutic targets of particular relevance to human PD.

Dopamine neurodegeneration induced by MPTP (1-methyl-4-phenyl-1,2,3,6-tetrahydropyridine) is currently the best available primate model of Parkinson's disease (PD; see refs. 1 and 2 for a current review). In adult monkeys, MPTP administration induces profound loss of dopamine neurons in the substantia nigra (SN) and motor impairments similar to those seen in idiopathic PD. The MPTP model, however, has two obvious limitations. First, MPTP-induced toxicity is a rapid, single-hit event, resulting in an acute onset of neurodegeneration and neurological symptoms. Second, the MPTP-affected dopamine neurons do not develop the progressive α-synucleinopathy (Lewy bodies and Lewy neuritis, in particular) that is the characteristic hallmark of idiopathic PD. There is thus an obvious need for a new primate model of PD where the pathogenetic mechanisms associated with α-synuclein (α-syn) toxicity and nigrostriatal degeneration can be studied in species close to man.

Previous studies have shown that the α-syn protein is a major component of the intraneuronal protein aggregates (Lewy bodies and Lewy neuritis) that are pathological hallmarks of the disease (3, 4). Moreover, point mutations in the α-syn gene have been shown to cause familiar PD (5, 6), suggesting that abnormal processing and/or function of α-syn may trigger the neurodegenerative process. Although α-syn is expressed in neurons throughout the nervous system, neurodegeneration in PD is remarkably selective and is most prominent in the dopaminergic neurons of the SN. Recent studies suggest that this selective vulnerability may be due to interaction of α-syn with intracellular dopamine, oxidative stress, and dopamine-dependent free radical damage (7–10). This interaction probably explains why dopaminergic neurons are affected by α-syn at expression levels that are nontoxic to other types of cells (10–13).

These *in vitro* data raise the possibility of generating transgenic models of PD by overexpression of the α-syn protein in the nigrostriatal dopamine neurons. This approach has given promising results in *Drosophila* (14). Nevertheless, the attempts made so far in mice, by using standard transgenic technology, have been disappointing. In the transgenic mouse strains generated to date, WT or mutated human α-syn have been expressed under neuron-specific promoters; although α-syn accumulation, α-syn-positive inclusions, and signs of neuronal injury have been widespread, no significant nigral pathology or cell loss has been detected in any of these mice (15–21). Recently, however, direct gene transfer by means of viral vectors has emerged as an interesting alternative to the standard transgenic approach. Recombinant adeno-associated virus (rAAV) and lentivirus vectors, in particular, are useful for this purpose because they transduce nondividing neurons with high efficiency in the CNS and are integrated and stably expressed without any signs of inflammatory or immune reactions (22, 23). These vector systems can be targeted to specific subregions of the CNS, and, in contrast to standard transgenic technology, they offer a transgenic approach that can be applied in adult animals and in other species than mice, such as rats and primates.

The rAAV vectors are of special interest in the context of PD because of their exceptionally high affinity for nigral dopamine neurons. In a previous study (24), we have shown that the rAAV vector system can be used to overexpress WT or mutant α-syn in the nigrostriatal neurons in adult rats, and that this overexpression is accompanied by the development of a pronounced α-synucleinopathy, including the appearance of α-syn-positive cytoplasmic inclusions and dystrophic neurites, a gradual loss of 30–80% of the nigral dopamine neurons, and PD-like behavioral improvements.

In the present study, we have applied this rAAV-α-syn vector construct to express human α-syn in the nigrostriatal dopamine neurons in a small nonhuman primate, the common marmoset. We report that the rAAV vector is equally effective in transducing the pars compacta neurons of the primate SN and show that overexpression of either WT or mutant human α-syn is sufficient to induce a PD-like neuropathology in the primate

This paper was submitted directly (Track II) to the PNAS office.

Abbreviations: MPTP, 1-methyl-4-phenyl-1,2,3,6-tetrahydropyridine; PD, Parkinson's disease; SN, substantia nigra; α-syn, α-synuclein; rAAV, recombinant adeno-associated virus; TH, tyrosine hydroxylase; VMAT-2, vesicular monoamine transporter-2; VTA, ventral tegmental area.

†To whom correspondence should be addressed. E-mail: deniz.kirik@mphy.lu.se.

www.pnas.org/cgi/doi/10.1073/pnas.0536383100

nigrostriatal system, accompanied by dopamine neuron cell loss and signs of motor impairments.

Experimental Protocols

rAAV Vectors. The rAAV-CBA-α-syn, rAAV-CBA-mu-α-syn, and rAAV-CBA-GFP vectors were produced by using a double transfection method with rAAV plasmids and a helper plasmid containing the necessary gene products normally provided by adenovirus (25), and purified as described (26). The final titers were 8.2×10^{11}, 1.4×10^{12}, and 1.5×10^{11} infectious units/ml, respectively, for the three vectors, as determined by an infectious center assay (27). The vectors express the transgene from a hybrid promoter consisting of an enhancer element from the cytomegalovirus promoter, followed by the chicken β-actin promoter containing a rabbit β-globin intron, termed CBA (28).

Animals and Surgery. All procedures were carried out under a project license in accord with the U.K. Animals (Scientific Procedures) Act 1986. Eight adult common marmosets (*Callithrix jacchus*), four males and four females, were used. All were laboratory-bred, aged 65–72 mo and weighed 340–380 g at the start of the experiment. The monkeys were housed in pairs with both members of the pair receiving the same type of rAAV vector injection. Two monkeys received injections of the rAAV vectors encoding the WT human α-syn, two received A53T mutated human α-syn, and four received a control vector encoding the GFP. In one of the rAAV-wt-α-syn injected animals, the injections failed; this animal was not included in the further analysis.

For surgery, the marmosets were anesthetized with alphaxalone-alphadone (Saffan; Schering–Plough; 0.5 ml of 12 mg/ml, i.m.). A supplementary dose of 0.3 ml Saffan was given during surgery if necessary. Infusions of 3 μl rAAV were made unilaterally at each of two sites in the right SN: anterior (A) 5.5, lateral (L) −2.5, and ventral (V) 6.6; and A 4.0, L −2.5, and V 6.6 [coordinates derived from the stereotaxic atlas of Stephan *et al.* (29)]. The injections were made at a rate of 0.25 μl/min by using a 29-gauge injection needle that was left in place for a further 4 min after each injection. After surgery, the monkeys were given an analgesic (Finadyne, Schering–Plough; 0.1 mg/kg, s.c.) and kept warm in an incubator until well enough to be returned to their home cage, usually later that day.

Behavior. Changes in motor behavior over time were monitored by amphetamine-induced rotation and a head position bias test (30, 31). In the latter test, the direction of the head relative to the body axis (ipsi- or contralateral to the injected side or straight ahead) was scored every second over three 1-min periods. The time difference (ipsi–contra) was used as a measure of head position bias. Tests were conducted preoperatively, at three weekly intervals and 16 wk after the AAV infusions.

Histology. The monkeys were perfused for histological analysis at 3–16 wk after vector injection. After premedication with 0.05 ml ketamine (Vetalar; Shering–Plough; 100 mg/ml, i.m.) and under deep anesthesia with 0.8 ml of sodium pentobarbitone (200 mg/ml, i.p.), the monkeys were perfused transcardially with 300 ml PBS, followed by 1,000 ml of 4% paraformaldehyde in PBS. The brains were placed in 4% paraformaldehyde solution for 24 h, after which they were transferred to 30% sucrose solution in PBS. Immunohistochemical stainings were performed on free-floating sections by using antibodies raised against tyrosine hydroxylase (TH; rabbit IgG, 1:250, Pel-Freez Biologicals), GFP (rabbit IgG, 1:20,000, Abcam, Cambridge, U.K.), vesicular monoamine transporter-2 (VMAT-2; rabbit IgG, 1:2,000, Chemicon), Hu (mouse IgG, 1:1,000, courtesy of S. A. Goldman, Cornell University, Ithaca, NY), and human α-syn (mouse IgG, 1:16,000, courtesy of V. M. Lee, University of Pennsylvania, Philadelphia). Incubation with primary antibodies was followed with the appropriate secondary antibodies conjugated to biotin, and avidin-biotin-peroxidase complex (ABC Elite, Vector Laboratories), visualized with 3,3′-diaminobenzidine, mounted on chrome-alum-coated glass slides and coverslipped. For colocalization of GFP and TH, incubation with anti-TH primary antibody was followed by donkey anti-rabbit antibody conjugated to Cy3 (red), and GFP was visualized using confocal microscopy by its native fluorescence in the green channel. An additional series of sections were stained for cresyl violet.

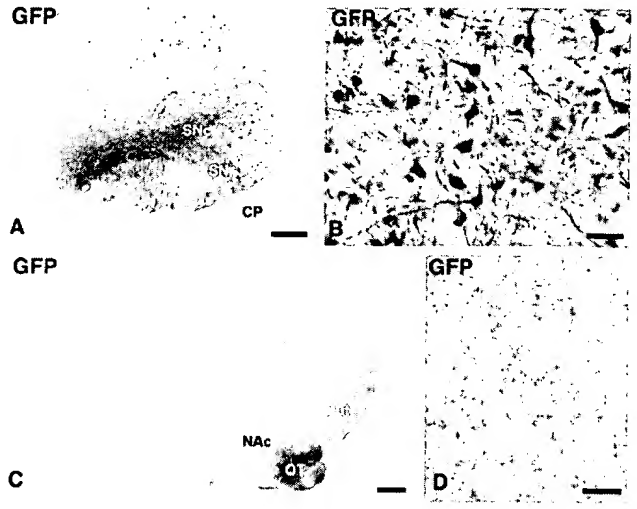

Fig. 1. Photomicrographs showing the expression of the GFP transgene in monkeys injected with the control vector. (*A* and *B*) GFP was expressed in the vast majority of the neurons in SN pars compacta, and some cells dorsally in the mesephalic tegmentum and ventrally in the SN pars reticulata (*A*). The transgenic GFP protein was transported along the axons of the nigrostriatal projection system to the caudate nucleus, putamen, and lateral olfactory tubercle, whereas the projections to the medial olfactory tubercle and the nc. accumbens were not labeled to the same extent (*C*; the noninjected control side is to the left). The density of GFP-expressing fibers in the striatum is shown in *D*. Scale bar in *A* = 0.5 mm; *B* and *D* = 50; *C* = 1 mm.

The total number of TH-positive and VMAT-2-positive neurons in the SN were estimated in separate series of sections according to the optical fractionator principle (32), by using the Olympus CAST system (Olympus Denmark A/S, Albertslund, Denmark). Every eighth section covering the entire extent of the SN was included in the counting procedure. The borders of the SN were defined as follows: the medial border between the ventral tegmental cell group and the pars compacta region was just lateral to the roots of the third nerve. At the most caudal level, the pars compacta was defined as the dense TH cell group ventral to the medial lemniscus and the retrorubral area. The TH-positive cells in the pars retriculata (and therefore dorsal to the cerebral peduncle) were included in the cell counts. This definition led typically to seven to eight sections per monkey being measured. A coefficient of error of <0.10 due to the estimation was accepted.

Results

The animals received injections of high-titer rAAV-α-syn and rAAV-GFP vectors unilaterally at two sites (2×3 μl) in the SN and were perfused at 3 wk ($n = 2$ from GFP group), and 16 wk ($n = 3$ from α-syn group and $n = 2$ from GFP group) after the transduction. In the rAAV-GFP-injected animals, 90–95% of the TH-positive cells were found to express GFP at all rostrocaudal levels throughout the SN, indicating that the nigral dopamine neurons were very efficiently transduced in the marmoset brain (Fig. 1 *A* and *B*). Most of the transduced cells in the

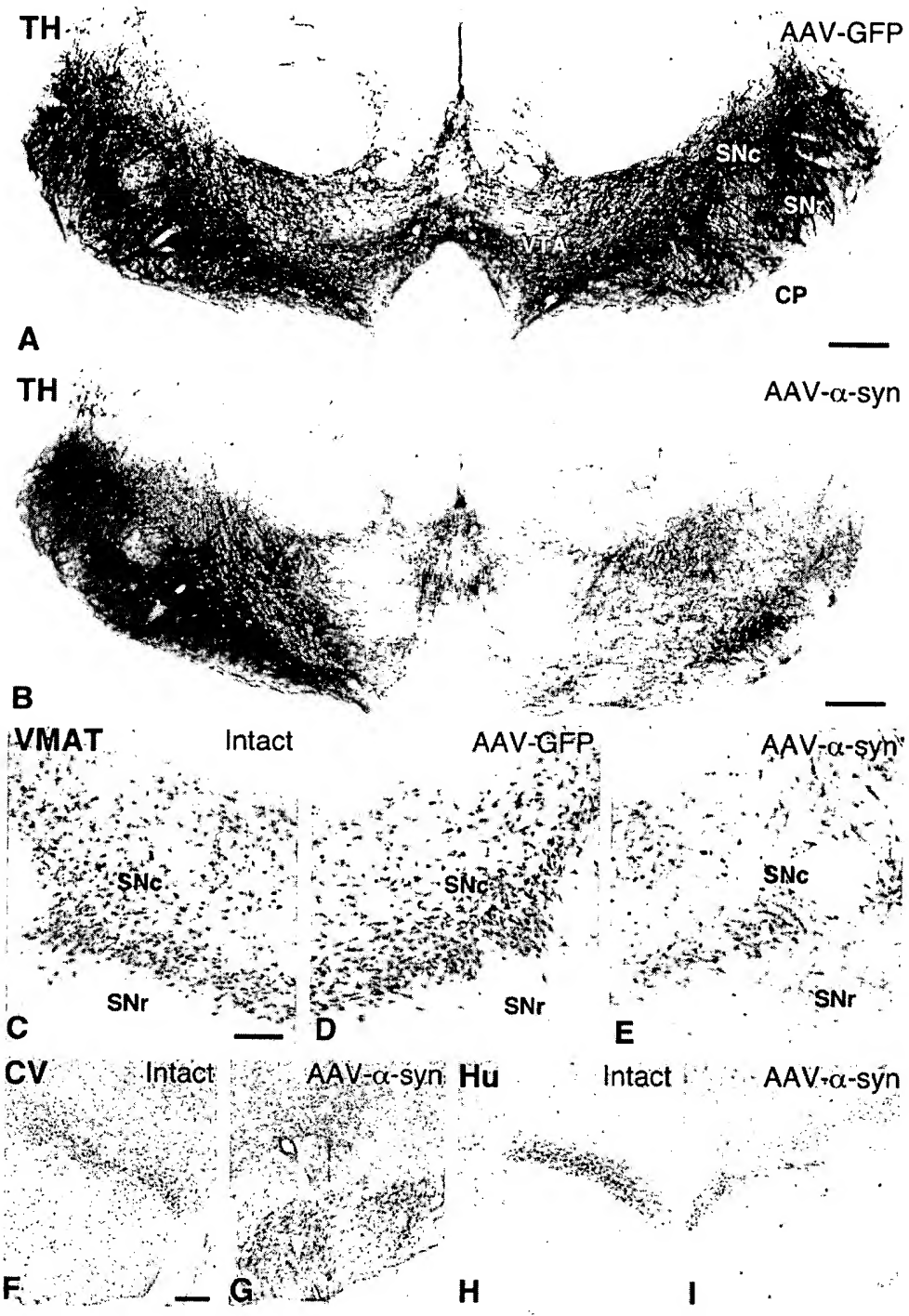

Fig. 2. Photomicrographs showing the TH-stained (*A* and *B*), VMAT-2-stained (*C–E*), cresyl violet-stained (*F* and *G*), and Hu-stained (*H* and *I*) sections at the level of SN. In the rAAV-GFP-treated animals, both TH (*A*) and VMAT (compare *C* and *D*) staining showed normal numbers and distribution of nigral dopaminergic cells. In the rAAV-α-syn-injected animals, by contrast, a clear loss of cells was seen both with TH (*B*) and VMAT-2 stainings (compare *C* and *E*). Scale bars in *A* and *B* = 0.5 mm; *C* = 300 μm (applies to *C–E*); *F* = 300 μm (applies to *F–I*). CP, cerebral peduncle; SNc, substantia nigra pars compacta; SNr, substantia nigra pars reticulate; VTA, ventral tegmental area.

SN were confined to the pars compacta, but some GFP-expressing cells were also found in the ventral tegmental area (VTA). In addition, GFP-expressing cells occurred in the SN pars reticulata, ventral to TH-positive cells, and dorsally in the mesencephalic tegmentum (Fig. 1*A*). In the two animals killed at 3 wk after rAAV-GFP injection, transgene expression was confined to the cell bodies and proximal axons within the SN pars compacta, as well as the dendrites extending into the pars reticulata. At 16 wk, transgene expression was maintained at a high level in the SN. In addition, anterogradely transported GFP protein could now be visualized also along the entire nigrostriatal pathway and in axon terminals throughout the striatum,

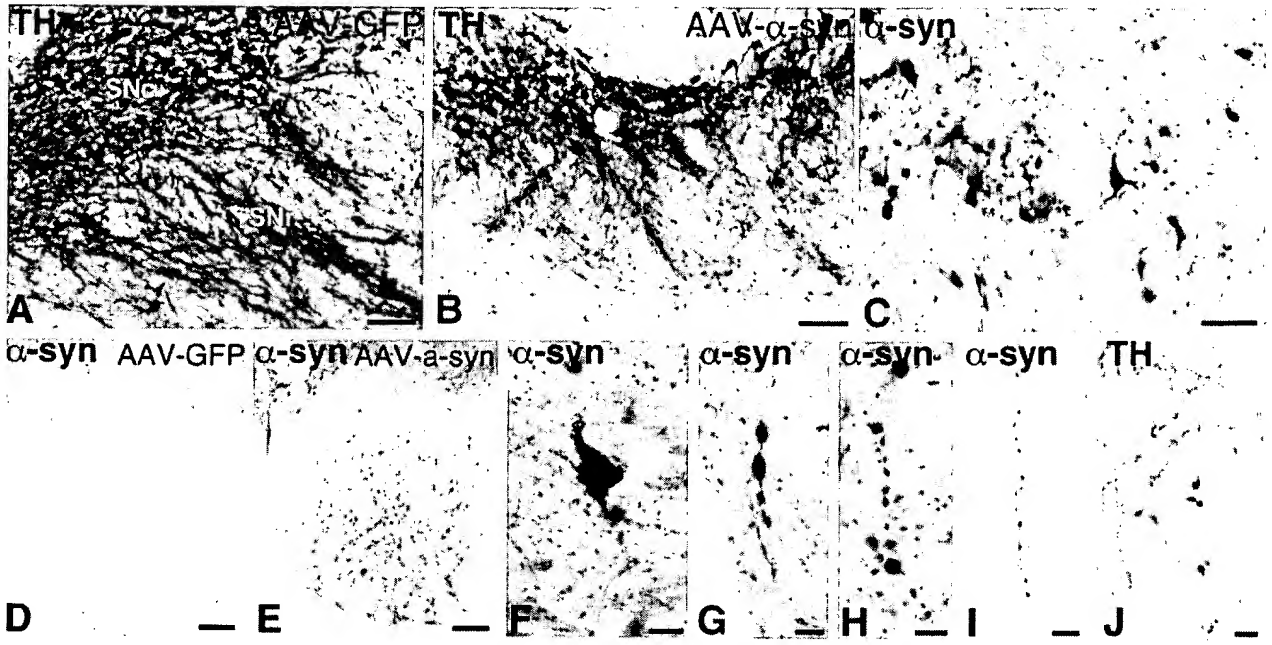

Fig. 3. Nigral degeneration in the rAAV-α-syn-injected animals. Pathological profiles in the SN were seen both with TH (*A*, *B*, and *J*) and α-syn immunoreactivity (*C–I*). Extensive cellular degeneration in the SN pars compacta, as visualized by TH immunoreactivity, also led to prominent dendritic abnormalities and loss of dendrites in the SN pars reticulata (*B* and *J*). Affected but surviving cells in SN pars compacta were shrunken (*C*) and contained numerous inclusions within the cytoplasm and proximal neurites (*F*), as well as in axons within pars compacta (*G* and *H*) and along the nigrostriatal bundle (*I*). Numerous pathological fibers with prominent inclusions were observed in the cerebral puduncle (cf. *D* and *E*). Scale bars in *A* and *B* = 0.1 mm; *C*, *I*, and *J* = 50 μm; *D* and *E* = 0.2 mm; *F*, *G*, and *H* = 25 μm.

including nc. accumbens and olfactory tubercle (Fig. 1 *C* and *D*). No signs of damage or degeneration could be detected in the GFP-transduced cells or their processes with any of the markers used (TH, VMAT-2, Hu, and cresyl violet; data not shown).

In animals injected with either of the two α-syn vectors, by contrast, there were clear signs of degeneration in the nigrostriatal dopamine neurons. The total number of TH-positive cells in the injected SN, as determined by stereology, was decreased by 32–61% in the three injected animals (from an average of 47,106 cells on the contralateral untreated side, to an average of 26,797 on the injected side; cf. Fig. 2 *A* and *B*). The same magnitude of cell loss (41–62%; from 43,034 cells on the control side to 23,214 cells on the injected side) was observed also in sections stained for the vesicular monoamine transporter, VMAT-2, arguing against the possibility of a selective down-regulation of TH protein in the α-syn-expressing cells (Fig. 2 *C–E*). The loss of dopaminergic cells was further supported by a similar reduction in the number of neuronal profiles within SN pars compacta in sections stained for the pan-neuronal marker, Hu, or with cresyl violet (Fig. 2 *F–J*). Cell death was most prominent in the central part of the SN but was seen at all rostrocaudal levels. Loss of TH- and VMAT-2-positive cells was observed also in the VTA, although of lesser magnitude than in SN. No such cell loss was observed in any of the rAAV-GFP-treated control monkeys (Fig. 2*A*).

Close examination of the SN transduced with either WT or mutant α-syn revealed signs of degeneration and ongoing pathology in the neurons of the pars compacta, including α-syn-positive cytoplasmic inclusions and granular deposits (Fig. 3*F*), α-syn- and TH-positive swollen, dystrophic and fragmented neurites (Fig. 3 *C*, *G*, and *H*), and shrunken, pyknotic perikarya with dense α-syn immunoreactivity (Fig. 3 *B* and *C*). Also, the dendrites projecting into the pars reticulata were severely damaged (cf. Fig. 3 *A*, *B*, and *J*), and α-syn- and TH-positive inclusions and swollen axons could be traced in large numbers along the nigrostriatal pathway (Fig. 3 *D* and *E*). Many of the surviving nigral cells, however, still expressing α-syn, had a normal intact appearance (Fig. 3*B*). In these cells, the α-syn immunoreactivity had an even, diffuse cytoplasmic distribution, suggesting that they had escaped the α-syn-induced toxic impact.

In the rAAV-α-syn-injected monkeys, degenerative changes in the axon terminals in the striatum could be visualized both with TH (Fig. 4*C*) and VMAT-2 antibodies (Fig. 4*D*). None of these changes were seen in the animals injected with the rAAV-GFP control vector (Fig. 4 *A* and *B*). A substantial loss of TH- and VMAT-2-positive fibers, in the order of 40–50%, occurred throughout the caudate nucleus and putamen, whereas the innervation in the ventral striatal and limbic regions, including nc. accumbens and the olfactory tubercle, was relatively spared (Fig. 4*C*; cf. Fig. 4 *E* and *F*). Swollen axons and pathological inclusions were observed in the remaining sparse TH-positive innervation in the striatum (Fig. 4 *F* and *G*), and also within the internal capsule (not shown).

In the behavioral tests, amphetamine-induced rotation did not show any consistent changes at any time point (data not shown). In the head position test, the preinjection average scores (±SEM) for the rAAV-α-syn and rAAV-GFP groups were +0.5 ± 5.4 and +9.4 ± 2.1 s, respectively. At 3 wk postinjection, i.e., at the time when transgene expression in the AAV-infected cells is fully developed (33–36), the animals in the rAAV-α-syn group showed a marked bias in the direction away from the injected hemisphere (−33.0 ± 5.7 s, as compared with +7.5 ± 2.1 s in the rAAV-GFP group). At 6 wk postinjection, this contralateral bias was reversed to an ipsilateral bias (+17.7 ± 1.7 s), as would be expected from animals with loss of dopamine innervation in the striatum. This bias persisted until the end of the experiment at 16 wk after transduction and was especially strong in two of the three rAAV-α-syn animals (+40.5, +22.3, −14 s, respectively), whereas the rAAV-GFP-injected animals showed no such bias (+5.5 and −7.3 s, respectively).

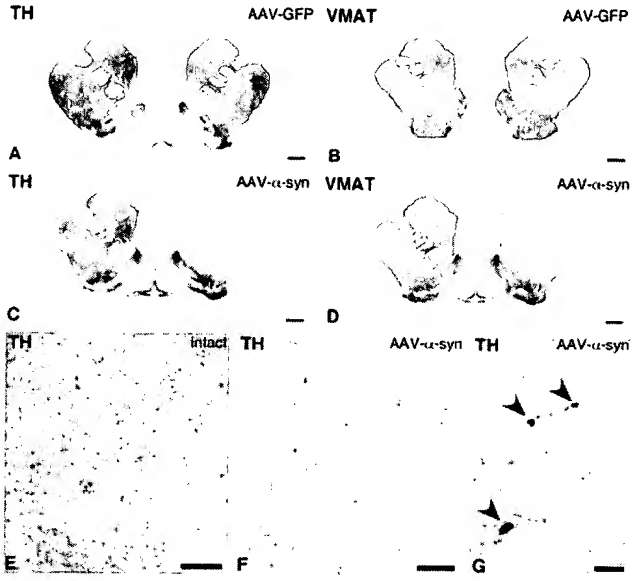

Fig. 4. Photomicrographs illustrating the axonal fiber innervation in the striatum visualized with TH (*A*, *B*, and *E–G*) and VMAT-2 (*B* and *D*) immunohistochemistry. Whereas expression of GFP protein did not alter the density of TH- and VMAT-2-positive fiber innervation in the striatum (*A* and *B*), the expression of α-syn led to prominent loss of fibers both in caudate nucleus and putamen in the transduced hemisphere, as compared with the contralateral intact side (*C* and *D*). Remaining TH-positive fibers in the α-syn-treated animals were sparse (compare *E* and *F*) and contained inclusions (*G*). Scale bars in *A–D* = 1 mm; *E* and *F* = 0.1 mm; *G* = 25 μm.

Discussion

The cellular changes induced by overexpression of α-syn in nigral dopamine neurons reproduces some of the cardinal neuropathological features of human PD, including α-syn-positive cytoplasmic inclusions and α-syn-positive swollen and dystrophic neurites, associated with degenerative changes in TH-positive axons and dendrites. In the rat, this α-synucleinopathy is a slowly developing process that starts at ≈3 wk after transduction and is fully developed by 2 mo. At that time point 30–80% of the nigral dopamine neurons and 25–90% of the striatal dopamine innervation are lost. A similar (30–60%) loss of TH- and VMAT-2-positive neurons in the SN, and a 40–50% reduction in TH- and VMAT-2-positive innervation throughout caudate nucleus and putamen was observed in the rAAV-α-syn-treated monkeys. Similar to idiopathic PD, the TH-positive neurons in the VTA and the associated innervation in limbic forebrain regions were relatively spared. These monkeys displayed a type of motor impairment, i.e., head position bias, that is compatible with the observed magnitude of nigral dopamine neuron cell loss. This side bias developed slowly, between 3 and 6 wk after transduction, and was maintained in two of the three animals until the end of the experiment (at 16 wk).

The nigral dopamine neurons seem to be particularly sensitive to α-syn overexpression. Interestingly, however, in both rats and monkeys, part of the transduced dopamine neurons survived long-term without any clear signs of damage, despite a maintained expression of the transduced α-syn protein, whereas others displayed signs of cellular and neuritic pathology suggestive of an ongoing neurodegenerative process. This variable vulnerability may be explained by the observation that α-syn toxicity is closely linked to the level of oxidative stress, and that dopamine neurons may be particularly sensitive due to interaction of α-syn with intracellular dopamine and dopamine-dependent oxidative mechanisms (7, 10, 11, 37, 38). It is worth noting that, with the current technique, the level of transgene expression will vary among the infected cells because neurons close to the injection site may receive more copies of the recombinant virus. However, it is likely that not only the level of α-syn expression but also the level of oxidative stress, which may vary from cell to cell, will determine the impact on the transduced cell. Previous *in vitro* studies (see, e.g., refs. 11, 38, and 39) have shown that the A53T and A30P mutants of human α-syn may be more toxic and make the transduced cells more vulnerable to oxidative stress, than the WT form. In the present model, as in some other *in vivo* experiments (14, 17, 19, 20, 24, 40), both the WT and the A53T mutant α-syn were highly toxic. In the absence of dose-response data, however, we cannot determine whether the two forms may differ in potency.

Neurodegeneration in PD is likely to depend on an interaction between α-syn (and the ubiquitin-proteasome pathway), oxidative stress, and mitochondrial impairment. Current animal models of PD successfully replicate the two latter mechanisms: 6-hydroxydopamine-induced toxicity mediated by oxidative damage, and MPTP- and rotenone-induced toxicity, mediated by chronic inhibition of mitochondrial complex I (1, 41). Targeted overexpression of α-syn in nigral dopamine neurons by rAAV vectors provides a new model of nigrostriatal α-synucleinopathy and α-syn-induced nigrostriatal neurodegeneration that will be a valuable complement to the existing ones. The advantage of this α-synucleinopathy model is that it is chronic and progressive, like human PD, and that it develops neuropathological features, in particular α-syn-positive inclusions and dystrophic neurites, that are similar (although not identical) to those seen in idiopathic PD. Moreover, neurodegeneration and behavioral impairments evolve over a relatively short period, 6–8 wk after transduction as determined in the rat (24), which is advantageous for experimental studies. Compared with standard transgenic mouse technology, vector-mediated transgenesis has a particular attraction, in that the transgenic protein can be delivered to adult animals at any time during the lifespan; that it can be targeted to specific subsets of neurons; that it can be applied uni- or bilaterally, as desired; and that it can be used also in primates. Viral vectors, and the new generation high-titer rAAV vectors in particular, provide new efficient tools for cell-specific, targeted transgenesis in the brain. The feasibility of using this approach in primates, as shown here, opens entirely new possibilities for the generation of transgenic primate models of neurodegenerative diseases, and for *in vivo* studies of pathogenetic mechanisms. Because rAAV vectors can be administered repeatedly to the same cells, they will be interesting also as tools for the expression of genes and intracellular factors that may block or interfere with critical pathogenetic processes (such as formation of toxic fibrils or protein aggregates in rAAV-α-syn-treated animals) and for the exploration of new molecular targets for therapeutic purposes.

We thank Ulla Jarl for expert technical assistance, Lyn Cummings for behavioral observations, the Department of Experimental Psychology at the University of Cambridge for use of the primate facility, the Powell Gene Therapy Center Vector Core Laboratory for production of the vectors, and Dr. Virginia M. Lee and Steven A. Goldman for generous supply of the α-synuclein and Hu antibodies, respectively. This study was supported by grants from the Swedish Medical Research Council (04X-3874 and 99-XG-13285), The Wellcome Trust (to L.E.A.), and the National Institutes of Health (PO1 NS36302, to N.M.).

1. Beal, M. F. (2001) *Nat. Rev. Neurosci.* **2,** 325–334.
2. Dawson, T., Mandir, A. & Lee, M. (2002) *Neuron* **35,** 219–222.
3. Spillantini, M. G., Schmidt, M. L., Lee, V. M., Trojanowski, J. Q., Jakes, R. & Goedert, M. (1997) *Nature* **388,** 839–840.
4. Goedert, M. (2001) *Nat. Rev. Neurosci.* **2,** 492–501.
5. Polymeropoulos, M. H., Lavedan, C., Leroy, E., Ide, S. E., Dehejia, A., Dutra, A., Pike, B., Root, H., Rubenstein, J., Boyer, R., *et al.* (1997) *Science* **276,** 2045–2047.
6. Kruger, R., Kuhn, W., Muller, T., Woitalla, D., Graeber, M., Kosel, S., Przuntek, H., Epplen, J. T., Schols, L. & Riess, O. (1998) *Nat. Genet.* **18,** 106–108.

7. Conway, K. A., Rochet, J. C., Bieganski, R. M. & Lansbury, P. T., Jr. (2001) *Science* **294,** 1346–1349.
8. McNaught, K. S., Olanow, C. W., Halliwell, B., Isacson, O. & Jenner, P. (2001) *Nat. Rev. Neurosci.* **2,** 589–594.
9. Przedborski, S., Chen, Q., Vila, M., Giasson, B. I., Djaldatti, R., Vukosavic, S., Souza, J. M., Jackson-Lewis, V. V., Lee, V. M. & Ischiropoulos, H. (2001) *J. Neurochem.* **76,** 637–640.
10. Xu, J., Kao, S. Y., Lee, F. J., Song, W., Jin, L. W. & Yankner, B. A. (2002) *Nat. Med.* **8,** 600–606.
11. Tabrizi, S. J., Orth, M., Wilkinson, J. M., Taanman, J. W., Warner, T. T., Cooper, J. M. & Schapira, A. H. (2000) *Hum. Mol. Genet.* **9,** 2683–2689.
12. Zhou, W., Hurlbert, M. S., Schaack, J., Prasad, K. N. & Freed, C. R. (2000) *Brain Res.* **866,** 33–43.
13. Junn, E. & Mouradian, M. M. (2002) *Neurosci. Lett.* **320,** 146–150.
14. Feany, M. B. & Bender, W. W. (2000) *Nature* **404,** 394–398.
15. Lee, M. K., Stirling, W., Xu, Y., Xu, X., Qui, D., Mandir, A. S., Dawson, T. M., Copeland, N. G., Jenkins, N. A. & Price, D. L. (2002) *Proc. Natl. Acad. Sci. USA* **99,** 8968–8973.
16. Giasson, B. I., Duda, J. E., Quinn, S. M., Zhang, B., Trojanowski, J. Q. & Lee, V. M. (2002) *Neuron* **34,** 521–533.
17. Masliah, E., Rockenstein, E., Veinbergs, I., Mallory, M., Hashimoto, M., Takeda, A., Sagara, Y., Sisk, A. & Mucke, L. (2000) *Science* **287,** 1265–1269.
18. Matsuoka, Y., Vila, M., Lincoln, S., McCormack, A., Picciano, M., LaFrancois, J., Yu, X., Dickson, D., Langston, W. J., McGowan, E., *et al.* (2001) *Neurobiol. Dis.* **8,** 535–539.
19. Kahle, P. J., Neumann, M., Ozmen, L., Muller, V., Jacobsen, H., Schindzielorz, A., Okochi, M., Leimer, U., van Der Putten, H., Probst, A., *et al.* (2000) *J. Neurosci.* **20,** 6365–6373.
20. van der Putten, H., Wiederhold, K. H., Probst, A., Barbieri, S., Mistl, C., Danner, S., Kauffmann, S., Hofele, K., Spooren, W. P., Ruegg, M. A., *et al.* (2000) *J. Neurosci.* **20,** 6021–6029.
21. Rathke-Hartlieb, S., Kahle, P. J., Neumann, M., Ozmen, L., Haid, S., Okochi, M., Haass, C. & Schulz, J. B. (2001) *J. Neurochem.* **77,** 1181–1184.
22. Samulski, R. J., Sally, M. & Muzyczka, N. (1999) in *The Development of Human Gene Therapy*, ed. Friedmann, T. (Cold Spring Harbor Lab. Press, Plainview, NY), pp. 131–170.
23. Naldini, L. & Verma, I. M. (1999) in *The Development of Human Gene Therapy*, ed. Friedmann, T. (Cold Spring Harbor Lab. Press, Plainview, NY), pp. 47–60.
24. Kirik, D., Rosenblad, C., Burger, C., Lundberg, C., Johansen, T. E., Muzyczka, N., Mandel, R. J. & Bjorklund, A. (2002) *J. Neurosci.* **22,** 2780–2791.
25. Hauswirth, W. W., Lewin, A. S., Zolotukhin, S. & Muzyczka, N. (2000) *Methods Enzymol.* **316,** 743–761.
26. Zolotukhin, S., Byrne, B. J., Mason, E., Zolotukhin, I., Potter, M., Chesnut, K., Summerford, C., Samulski, R. J. & Muzyczka, N. (1999) *Gene Ther.* **6,** 973–985.
27. McLaughlin, S. K., Collis, P., Hermonat, P. L. & Muzyczka, N. (1988) *J. Virol.* **62,** 1963–1973.
28. Xu, L., Daly, T., Gao, C., Flotte, T. R., Song, S., Byrne, B. J., Sands, M. S. & Ponder, K. P. (2001) *Hum. Gene Ther.* **12,** 563–573.
29. Stephan, H., Baron, G. & Schwerdtfeger, W. K. (1980) (Springer, Berlin).
30. Annett, L. E., Rogers, D. C., Hernandez, T. D. & Dunnett, S. B. (1992) *Brain* **115,** 825–856.
31. Annett, L. E., Smyly, R. E., Henderson, J. M., Cummings, R. A., Kendall, A. L. & Dunnett, S. B. (2000) in *Innovative Animal Models of Central Nervous System Disease: From Molecule to Therapy*, eds. Emerich, D. F., Dean, R. L. & Sandberg, P. (Humana, Totowa, NJ), pp. 171–186.
32. West, M. J. (1999) *Trends Neurosci.* **22,** 51–61.
33. Mandel, R. J., Rendahl, K. G., Snyder, R. O. & Leff, S. E. (1999) *Exp. Neurol.* **159,** 47–64.
34. Mandel, R. J., Snyder, R. O. & Leff, S. E. (1999) *Exp. Neurol.* **160,** 205–214.
35. Lo, W. D., Qu, G., Sferra, T. J., Clark, R., Chen, R. & Johnson, P. R. (1999) *Hum. Gene Ther.* **10,** 201–213.
36. Ferrari, F. K., Samulski, T., Shenk, T. & Samulski, R. J. (1996) *J. Virol.* **70,** 3227–3234.
37. Giasson, B. I., Jakes, R., Goedert, M., Duda, J. E., Leight, S., Trojanowski, J. Q. & Lee, V. M. (2000) *J. Neurosci. Res.* **59,** 528–533.
38. Kanda, S., Bishop, J. F., Eglitis, M. A., Yang, Y. & Mouradian, M. M. (2000) *Neuroscience* **97,** 279–284.
39. Ostrerova, N., Petrucelli, L., Farrer, M., Mehta, N., Choi, P., Hardy, J. & Wolozin, B. (1999) *J. Neurosci.* **19,** 5782–5791.
40. Lo Bianco, C., Ridet, J. L., Schneider, B. L., Deglon, N. & Aebischer, P. (2002) *Proc. Natl. Acad. Sci. USA* **99,** 10813–10818.
41. Betarbet, R., Sherer, T. B., MacKenzie, G., Garcia-Osuna, M., Panov, A. V. & Greenamyre, J. T. (2000) *Nat. Neurosci.* **3,** 1301–1306.

Exhibit D

ORIGINAL CONTRIBUTION

Frequency of Tau Gene Mutations in Familial and Sporadic Cases of Non-Alzheimer Dementia

Parvoneh Poorkaj, PhD; Murray Grossman, MD; Ellen Steinbart, MA; Haydeh Payami, PhD; Adele Sadovnick, PhD; David Nochlin, MD; Takeshi Tabira, MD; John Q. Trojanowski, MD, PhD; Soo Borson, MD; Douglas Galasko, MD; Stephen Reich, MD; Bruce Quinn, MD, PhD; Gerard Schellenberg, PhD; Thomas D. Bird, MD

Background: Mutations in the tau gene have been reported in families with frontotemporal dementia (FTD) linked to chromosome 17. It remains uncertain how commonly such mutations are found in patients with FTD or non-Alzheimer dementia with or without a positive family history.

Objective: To determine the frequency of tau mutations in patients with non-Alzheimer dementia.

Patients and Methods: One hundred one patients with non-Alzheimer, nonvascular dementia, most thought to have FTD. Of these, 57 had a positive family history of dementia. Neuropathologic findings were available in 32. The tau gene was sequenced for all exons including flanking intronic DNA, portions of the 3′ and 5′ untranslated regions, and at least 146 base pairs in the intron following exon 10.

Results: Overall, the frequency of the tau mutations was low, being 5.9% (6/101) in the entire group. No mutations were found in the 44 sporadic cases. However, 6 (10.5%) of the 57 familial cases and 4 (33%) of the 12 familial cases with tau pathologic findings had mutations in the tau gene. The most common mutation was P301L.

Conclusions: We conclude that tau mutations are uncommon in a neurology referral population with non-Alzheimer dementia, even in those with a clinical diagnosis of FTD. However, a positive family history and/or tau pathologic findings increase the likelihood of a tau mutation. There must be other genetic and nongenetic causes of FTD and non-Alzheimer dementia, similar to the etiologic heterogeneity present in Alzheimer disease.

Arch Neurol. 2001;58:383-387

FRONTOTEMPORAL dementia (FTD) has been increasingly recognized as a common form of non–Alzheimer disease (AD) dementia that is clinically characterized by behavioral problems predominating over memory loss and frontal and temporal lobar cortical atrophy.[1] A familial subtype of FTD, often with parkinsonian features, has been linked to chromosome 17,

For editorial comment see page 351

and several mutations in the tau gene have been discovered to segregate with the disease in most of these families.[2-6] Because FTD and other non-AD dementias are relatively common, especially in the presenile age group (younger than 65 years), it is important to determine the frequency of tau mutations in this population. Thus far, only 2 studies have addressed this issue. Rizzu et al,[7] in an FTD population from the Netherlands, found that 17.8% of cases had a tau mutation and 43% of cases with a positive family history had a tau mutation. Houlden et al[8] studied non-AD dementia cases from Minnesota and the United Kingdom. They found no tau mutations in 71 non-AD cases, whereas 9.4% to 13.6% of those with pathologic findings of FTD had tau mutations. We report herein the largest series to date from North America of FTD and non-AD cases of dementia evaluated for mutations in the tau gene.

The affiliations of the authors appear in the acknowledgment section at the end of the article.

RESULTS

The results are summarized in **Table 2** and **Table 3**. Fifty-seven cases were familial and 44 were sporadic. There were no differences in the mean ages at onset for the familial and sporadic cases. Eighteen of the familial cases and 14 of the sporadic cases had autopsies, 22 of which showed some form of tau pathologic changes. Twenty cases had neurofibrillary tangles and 9 had Pick bodies. Six tau mutations were discovered in the total

PATIENTS AND METHODS

We ascertained 101 unrelated index patients with non-AD, nonvascular dementia who were thought most likely to have FTD or some variant of FTD. The majority of these were ascertained from the Neurology and Alzheimer's Disease Research Center clinics at the University of Washington, Seattle, and the University of Pennsylvania, Philadelphia. Additional individual cases were referred by several neurologists (see acknowledgments). Criteria for inclusion were initial behavioral problems exceeding memory loss, often with neuroimaging or neuropathologic evidence of lobar atrophy.[1] Exclusion criteria were a diagnosis of typical AD, progressive supranuclear palsy, Parkinson disease, alcoholism, vascular dementia, and Lewy body dementia. Most of the patients had a clinical diagnosis of FTD conforming to the guidelines of Neary et al.[1] Family histories were available for 86 cases, and those having a first-degree relative with dementia were considered familial. Subjects with a negative family history or no available family history were considered sporadic. These cases do not represent a random or community-based sample but have a bias of ascertainment toward unusual dementia referred to special academic research units. Subjects participated through informed consent protocols approved by the relevant institutional review boards.

Neuropathologic examination was performed on 32 brains and included staining of microscopic sections from neocortex, hippocampus, basal ganglia, cerebellum, and brainstem with hematoxylin-eosin, Bielschowsky silver, tau-2, paired helical filament, and Aβ-amyloid. Pathologic changes related to tau were defined as any tau-positive cytoplasmic inclusion, which included neurofibrillary tangles and Pick bodies.[3] Eight cases subjected to autopsy met criteria for dementia lacking distinctive histopathologic features.[9]

The initial family (BK or Seattle A) with a tau mutation discovered at the University of Washington was excluded from this study.[3]

DNA samples from affected persons in the families with dementia were prepared from peripheral leukocytes as previously described.[10,11] Primer pairs for each exon from tau were used to amplify 200 ng of patient genomic DNA in 50-μL reactions (35 cycles) containing 1X polymerase chain reaction buffer, 200 ng of each primer, 2.5 U of Taq DNA polymerase (Promega Corp, Madison, Wis), and 400-μmol/L deoxynucleoside triphosphatase (Perkin-Elmer, Norwalk, Conn) (**Table 1**). Polymerase chain reaction products were subjected to electrophoresis with the use of 2.5% agarose/0.1× TAE (Tris-acetate-ethylenediaminetetraacetate) gels and the appropriate fragments purified with a DNA purification kit (Bio 101 Inc, La Jolla, Calif). The purified fragments were sequenced automatically with dye terminator cycle sequencing (TaqFS DNA polymerase or Big Dye Terminator RR Mix; Perkin-Elmer), and an ABI 373 or 377 DNA Sequencer (Applied Biosystems, Foster City, Calif).

Primer pairs for amplification and sequencing tau have been described previously.[4] New primers were designed for 9 of the 11 exons to sequence deeper into the introns (Table 1) and were used for sequencing in approximately 50 of the 100 patients. Both strands of the tau gene were sequenced for all exons, including at least 7 base pairs (bp) of flanking intronic DNA, 50 bp of the 5′-untranslated region, and 70 bp of the 3′ untranslated region. For all cases, more than 146 bp of flanking sequence for intron 10 were analyzed. DNA samples were available from a panel of 96 unrelated normal control subjects to determine whether any changes occurred in the general population.

group (6/101; 5.9%), the most common of which was P301L (proline-to-leucine substitution at nucleotide 301) (3/6). Other mutations were L284L (leucine-to-leucine silent substitution at nucleotide 284), S305N (serine-to-asparagine substitution at nucleotide 305), and E10+16 (nucleotide substitution at position +16 in intron 10). The detailed descriptions of these families have been reported elsewhere.[4,12-15] Fifty-seven patients had a positive family history of dementia in at least 1 first-degree relative, and all 6 tau mutations came from this group (10.5%). No tau mutations were found in the 44 sporadic cases. There were 4 tau mutations in the familial cases with neuropathologic features (22%), and all 4 came from the familial group with tau pathologic features (4/12; 33%). Of all 22 cases in the total familial and sporadic groups with tau pathologic features at autopsy, 4 (18%) were found to have tau mutations. None of the 9 sporadic cases with Pick bodies and none of the 8 cases of dementia lacking distinctive histopathologic features had tau mutations.

Table 4 lists the 22 normal polymorphisms found in the tau gene in the control samples. Nine of these polymorphisms have been previously published and 13 are new. This list will be of value to other investigators searching for mutations in tau.

COMMENT

These results demonstrate that mutations in the tau gene are a relatively uncommon cause of FTD and non-AD, nonvascular dementia in a neurology referral population. The frequency of mutations in this population is approximately 6%, and all were found in subjects with a positive family history. Frontotemporal dementia can be familial (45% in the study by Chow et al[18]). A positive family history of dementia and/or evidence of tau-related neuropathologic features greatly increases the probability of a tau mutation (10% to 30%). However, even familial cases and cases with tau pathologic features may not have demonstrable mutations.

One caveat concerning these results is that no group, including our own, has performed a complete exhaustive screen of the entire tau gene including all regulatory, noncoding, and intronic regions. It is conceivable that rare disease-related mutations lie in these regions, but the number of such mutations is likely to be small. One possible example of this phenomenon is the hereditary dysphasic dementia 2 (HDD2) family linked to chromosome 17 but having no demonstrable tau mutation.[19] The tau gene has a large number of polymorphisms (Table 4) that occur fairly frequently in the general population

Table 1. Tau Exon Primers Used for Genomic PCR Amplifications and Sequencing*

Tau Exon/Primer	Primer Sequence 5′-3′	Primer Position Relative to Exon	Product Size, nt	Annealing Temperature, °C
1EF	GCCAACTGTTAGAGAGGGTAGC	−136	...	...
1ER	GTGTCTGGCCATTATCTCACTGC	+183	469	60
2EF	TTGCCTCAGGTGGCACCACTAGC	−293	...	...
2ER	TGGCTGCTCTGGGACCTACTGGC	+345	725	60
3BF	CACTGCAGCGTTTACACAGG	−266	...	...
3BR	CTGTCACAGGTCAGCTGGG	+68	422	60
4BF	AGACACAGCCTCCACAACC	−360	...	...
4BR	CTCTTTCTATATCTGAGTAGCC	+165	592	60
5BF	TGTTGATACTAACAATGCGAGG	−181	...	...
5BR	AAGCACTTTAAATGACAGC	+132	369	60
7BF	CAGACACTAGTGGCATCTAGG	−148	...	...
7BR	AGGCAATGAAGACTCCAGTGC	+152	427	60
9EF	CCACACAGCTTGTTGGAGCC	−325	...	...
9ER	TCACAGTGTAGTGGAGAGCC	+233	824	60
10GF	GTCTAGCCAGGTGTGAGTGG	−426	...	...
10CR	GGCTACATTCACCCAGAGG	+146	665	60
11EF	TGCTTCTCATTGAGTTACACC	−113	...	...
11ER	TTGTCTTGGGCAGCATGGCC	+212	417	60
12EF	TTGGCCCTGGTTCAAGTCC	−218	...	...
12ER	CCCACTGGATGCTGCTGAG	+151	472	60
13F	ACTTCATCTCACCCTCCCTC	−37	...	...
13R	CCTCTCCTTCTCCCTCTT	352	597	60

**PCR indicates polymerase chain reaction; nt, nucleotide; F, forward; ellipses, not applicable; and R, reverse.*

Table 2. Tau Mutations in 101 Index Cases With FTD or Non-AD Dementia*

	No. of Subjects	Age, Mean ± SD, y		Tau Mutations, No. (%)
		At Onset	At Death	
Familial	57	57.7 ± 10.5	68.0 ± 10.0	6 (10.5)
With neuropathologic findings	18	55.4 ± 11.1	67.7 ± 10.2	4 (22)
With tau-related pathologic findings	12	58.6 ± 9.9	69.8 ± 9.5	4 (33)
Without neuropathologic findings	39	59.0 ± 10.0	73†	2 (5.1)
Sporadic	44	54.7 ± 11.8	67.9 ± 7.4	0
With neuropathologic findings	14	60.4 ± 9.4	67.9 ± 7.4	0
With tau-related pathologic findings	9	62.1 ± 9.9	69.3 ± 7.0	0
Without neuropathologic findings	30	52.1 ± 11.9	No deaths	0
All cases	**101**			6 (5.9)

**FTD indicates frontotemporal dementia; AD, Alzheimer disease.*
†Only 1 death.

and are not likely to be disease related, but may be difficult to interpret in small focused studies. One exception appears to be the A0 polymorphism, which shows a consistent and significant association with progressive supranuclear palsy.[20]

Even though no tau mutations have yet been found in a sporadic case of FTD, an occasional case is likely to be discovered. The most common explanations for such a phenomenon would be nonpaternity, a new mutation, decreased penetrance in other family members, or early presymptomatic death of a mutation-carrying parent.[21]

Our results are similar to those of Houlden et al,[8] who evaluated cases from Minnesota and the United Kingdom. They, too, found no mutations in sporadic non-AD cases and a 9.4% to 13.6% frequency of mutations in cases with tau pathologic features. Rizzu et al[7] found a higher frequency of tau mutations in an FTD population in the Netherlands (17.8% overall and 43% in the familial cases). These latter results may reflect the presence of a few large families with FTD linked to chromosome 17 in the relatively small population of the Netherlands. Nevertheless, all investigators have documented many FTD cases without tau mutations.

These results have important practical implications. Neurologists and/or clinical laboratories screening patients with dementia for tau mutations will have a low yield of positive results, unless there is a strong family history of dementia and tau-related neuropathologic findings. However, discovering a patient with a tau mutation has utmost importance to the family in providing genetic counseling.

Mutations in the tau gene appear to cause neuronal dysfunction and death by at least 2 mechanisms.[22,23] One is by altering the ability of tau to bind microtubules. The

Table 3. Six Families With Tau Mutations*

Family	Mutation†	Mean Age (Range), y		Clinical Diagnosis	Neuropathologic Findings	Mutation Effect	References
		At Onset	At Death				
GAA	P301L	49.5 (41-57)	56.3 (46-63)	FTD, atypical dementia, atypical PD	NFT, tau + inclusions	Abnormal MTB	4, 12
LBL	P301L	61.0 (56-67)	68.3 (56-77)	FTD, atypical dementia	Ballooned neurons, NFT	Abnormal MTB	4, 12
OREL	P301L	64.3 (57-75)	72.3 (65-80)	FTD	NA	Abnormal MTB	4, 12
EKR	E10+16	48 (48-55)	65 (65-75)	FTD, atypical dementia	NA	Abnormal splice E10	Present study, 15
LKL	L284L	51.8 (47-52)	62.0 (57-71)	FTD, AD	NFT, neuritic amyloid plaques	Abnormal splice E10	14
TAB	S305N	36.7 (29-38)	38.0 (35-41)	FTD, atypical dementia	NFT	Unknown	13

*FTD indicates frontotemporal dementia; PD, Parkinson disease; AD, Alzheimer disease; NFT, neurofibrillary tangles; NA, no pathologic findings available; MTB, microtubule binding; and splice E10, splicing of exon 10.
†See the "Results" section for an explanation of the mutations.

Table 4. Polymorphisms in the Tau Gene*

Location	Polymorphic Nucleotide	Primer Pair	Position Relative to Exon of Primer Pair	Codon†	References
5'UTR	A/G	1EF/1ER	-13 from ATG		4, 7, 16
I1	C/T	2EF/2ER	+18		7, 16
I2	C/G	3BF/3BR	-163		Present study
I2	T/G	3BF/3BR	-162		Present study
I2	A/G	3BF/3BR	-139		Present study
I3	A/G	3BF/3BR	+9		7, 17
I3	T/A	4BF/4BR	-103		Present study
I3	A/T	4BF/4BR	-94		Present study
I4	A insertion	4BF/4BR	+45		Present study
I5	T/C	5EF/5ER	-72		Present study
E7	G/A	7EF/7ER		176	7
I8	G/A	9EF/9ER	-26		Present study
E9	A/G	9EF/9ER		227	7, 16
E9	T/C	9EF/9ER		255	4, 7, 16
E9	G/A	9EF/9ER		270	7
I9	G/A	9EF/9ER	+103		Present study
I10	G/A	10GF/10CR	+29		Present study
I11	G/A	11EF/11ER	+34		7, 16, 17
3'UTR	T/C	13F/13R	+34		4, 16
3'UTR	AAT deletion	13F/13R	+76		Present study
3'UTR	T insertion	13F/13R	+250		Present study
3'UTR	C insertion	13F/13R	+321		Present study

*UTR indicates untranslated region; I, intron; E, exon; F, forward; and R, reverse.
†Numbering based on the full-length tau sequence with exons 2, 3, and 10.

other is by altering the normal 1:1 ratio of 3 repeat and 4 repeat tau by abnormal splicing of exon 10. Both types of mutations were found in the present study (Table 3). The abnormal microtubule binding, perturbed isoform ratio, and cytoplasmic protein aggregation produce a delayed-onset, progressive dementing illness, but the pathogenesis of this disorder requires much further investigation.

Finally, the relationship of tau gene mutations to the pathogenesis of AD remains intriguing. Most brains from cases with tau mutations have no amyloid plaque pathologic features, but there have been a few exceptions, including 1 of the cases in this series (family LKL, reported previously).[14,24,25] Because AD, by definition, has tau pathologic findings (neurofibrillary tangles), the interactions between tau and amyloid require much more attention and elucidation.

We conclude that, although mutations in the tau gene represent a powerful insight into the pathogenesis of neurodegenerative diseases, the frequency of such mutations in the general population of non-AD dementia is small. Such mutations are more common in cases with an FTD phenotype with a positive family history and neuropathologic evidence of abnormal tau inclusions. There must be additional causes of the FTD syndrome, including other genes involved in the familial cases. This evidence of heterogeneity in FTD is remarkably similar to that found in AD, where 3 genes (amyloid precursor protein and presenilins 1 and 2) cause some instances of early-onset familial cases and there is a genetic risk factor (apolipoprotein E), but the largest numbers of both familial and sporadic cases still have no known cause.

Accepted for publication June 12, 2000.

From the Departments of Medicine (Drs Poorkaj, Schellenberg, and Bird and Ms Steinbart), Neurology (Drs Schellenberg and Bird), Pathology (Dr Nochlin), and Psychiatry (Drs Borson, Schellenberg, and Bird), University of Washington, Seattle; Geriatrics Research Education Clinical Center, Puget Sound Veterans Affairs Health Care System, Seattle (Drs Poorkaj, Schellenberg, and Bird and Ms Steinbart); Departments of Neurology and Pathology, University of Pennsylvania, Philadelphia (Drs Grossman and Trojanowski); Department of Genetics, Oregon Health Sciences University, Portland (Dr Payami); Department of Medical Genetics, University of British Columbia, Vancouver (Dr Sadovnick); National Institute of Neuroscience, Tokyo, Japan (Dr Tabira); Department of Neurology, University of California, San Diego (Dr Galasko); Department of Neurology, The Johns Hopkins University School of Medicine, Baltimore, Md (Dr Reich); and Department of Cognitive Neurology and AD Center, Northwestern University, Chicago, Ill (Dr Quinn).

This study was supported by grants AG05136, AG10124, and AG17586 from the National Institute on Aging, Bethesda, Md, and Veterans Affairs Medical Research Funds, Washington, DC.

We thank the following physicians who contributed single cases: Michael Conneally, PhD; John Ebans, MD; William Jagust, MD; John Kamholz, MD; Andrew Kertesz, MD; Walter Koroshetz, MD; Maureen Leehey, MD; John Morris, MD; David Munoz, MD; Phillip Swanson, MD, PhD; Armistead Williams, MD; and Minoru Yasada, MD, PhD.

Corresponding author and reprints: Thomas D. Bird, MD, Geriatrics Research Education Clinical Center 182 B, VA Medical Center, 1660 S Columbian Way, Seattle, WA 98108 (e-mail: tomnroz@u.washington.edu).

REFERENCES

1. Neary D, Snowden J, Gustafson, L et al. Frontotemporal lobar degeneration: a consensus on clinical diagnostic criteria. *Neurology.* 1998;51:1546-1554.
2. Foster NL, Wilhelmsen K, Sima AF, et al. Frontotemporal dementia and parkinsonism linked to chromosome 17: a consensus conference. *Ann Neurol.* 1997; 41:706-715.
3. Spillantini MG, Bird TD, Ghetti B. Frontotemporal dementia and parkinsonism linked to chromosome 17: a new group of tauopathies. *Brain Pathol.* 1998;8: 387-402.
4. Poorkaj P, Bird TD, Wijsman E, et al. Tau is a candidate gene for chromosome 17 frontotemporal dementia. *Ann Neurol.* 1998;43:815-825.
5. Hutton M, Lendon C, Rizzu P, et al. Association of missense and 5'-splice-site mutations in tau with the inherited dementia FTDP-17. *Nature.* 1998;393:702-705.
6. Spillantini MG, Murrell JR, Goedert M, et al. Mutation in the tau gene in familial multiple system tauopathy with presenile dementia. *Proc Natl Acad Sci U S A.* 1998;95:7737-7741.
7. Rizzu P, Van Swieten JC, Joosse M, et al. High prevalence of mutations in the microtubule-associated protein tau in a population study of frontotemporal dementia in the Netherlands. *Am J Hum Genet.* 1999;64:414-421.
8. Houlden H, Baker M, Adamson J, et al. Frequency of tau mutations in three series of non-Alzheimer's degenerative dementia. *Ann Neurol.* 1999;46:243-248.
9. Knopman DS, Mastri AR, Frey WH, et al. Dementia lacking distinctive histologic features: a common non-Alzheimer degenerative dementia. *Neurology.* 1990; 40:251-256.
10. Levy-Lahad E, Poorkaj P, Wang K, et al. Genomic structure and expression of STM2, the chromosome 1 familial Alzheimer's disease gene. *Genomics.* 1996; 34:198-204.
11. Bird TD, Wijsman EM, Nochlin D, et al. Chromosome 17 and hereditary dementia: linkage studies in three non-Alzheimer families and kindreds with late-onset FAD. *Neurology.* 1997;48:949-954.
12. Bird TD, Nochlin D, Poorkaj P, et al. A clinical pathological comparison of three families with frontotemporal dementia and identical mutations in the tau gene (P301L). *Brain.* 1999;122:741-756.
13. Iijima M, Tabira T, Poorkaj P, et al. A distinct familial presenile dementia with a novel missense mutation in the tau gene. *Neuroreport.* 1999;10:497-501.
14. D'Souza I, Poorkaj P, Hong M, et al. Missense and silent tau gene mutations cause frontotemporal dementia with parkinsonism–chromosome 17 type, by affecting multiple alternative RNA splicing regulatory elements. *Proc Natl Acad Sci U S A.* 1999;96:5598-5603.
15. Goedert M, Spillantini MG, Crowther RA, et al. Tau gene mutation in familial progressive subcortical gliosis. *Nat Med.* 1999;5:454-457.
16. Baker M, Litvan I, Houlden H, et al. Association of an extended haplotype in the tau gene with progressive supranuclear palsy. *Hum Mol Genet.* 1999;4:711-715.
17. Bullido MJ, Aldudo J, Frank A, et al. A polymorphism in the tau gene associated with risk for Alzheimer's disease. *Neurosci Lett.* 2000;278:49-52.
18. Chow T, Miller B, Hayashi V, Geschwind DH. Inheritance of frontotemporal dementia. *Arch Neurol.* 1999;56:817-822.
19. Lendon CL, Lynch T, Norton J, et al. Hereditary dysphasic disinhibition dementia: a frontotemporal dementia linked to 17q21-22. *Neurology.* 1998;50:1546-1555.
20. Conrad C, Amano N, Andreadis A, et al. Differences in dinucleotide repeat polymorphism in the tau gene between Caucasian and Japanese populations: implication for progressive supranuclear palsy. *Neurosci Lett.* 1998;250:135-137.
21. Bird TD. Sporadic cases of possible genetic diseases: to test or not to test. *Arch Neurol.* 2000;57:309-310.
22. Hong M, Zhukareva V, Vogelsberg-Ragalia V, et al. Mutation-specific functional impairments in distinct tau isoforms of hereditary FTDP-17. *Science.* 1998;282: 1914-1917.
23. Clark L, Poorkaj P, Wszolek Z, et al. Pathogenic implications of mutations in the tau gene in pallido-ponto-nigral degeneration and related neurodegenerative disorders linked to chromosome 17. *Proc Natl Acad Sci U S A.* 1998;95:13103-13107.
24. Van Swieten JC, Stevens M, Rosso SM, et al. Phenotypic variation in hereditary frontotemporal dementia with tau mutations. *Ann Neurol.* 1999;46:617-626.
25. Dark F. A family with autosomal dominant, non-Alzheimer's presenile dementia. *Aust N Z J Psychiatry.* 1997;31:139-144.

Examples of references of characterized tau mutants.

Hoenicka J, Perez M, Perez-Tur J, Barabash A, Godoy M, Vidal L, Astarloa R, Avila J, Nygaard T, de Yebenes JG.
The tau gene A0 allele and progressive supranuclear palsy.
Neurology. 1999 Oct 12;53(6):1219-25.
PMID: 10522876 [PubMed - indexed for MEDLINE]

Yen SH, Hutton M, DeTure M, Ko LW, Nacharaju P.
Fibrillogenesis of tau: insights from tau missense mutations in FTDP-17.
Brain Pathol. 1999 Oct;9(4):695-705. Review.
PMID: 10517508 [PubMed - indexed for MEDLINE]

Yasuda M, Kawamata T, Komure O, Kuno S, D'Souza I, Poorkaj P, Kawai J, Tanimukai S, Yamamoto Y, Hasegawa H, Sasahara M, Hazama F, Schellenberg GD, Tanaka C.
A mutation in the microtubule-associated protein tau in pallido-nigro-luysian degeneration.
Neurology. 1999 Sep 11;53(4):864-8.
PMID: 10489057 [PubMed - indexed for MEDLINE]

Arawaka S, Usami M, Sahara N, Schellenberg GD, Lee G, Mori H.
The tau mutation (val337met) disrupts cytoskeletal networks of microtubules.
Neuroreport. 1999 Apr 6;10(5):993-7.
PMID: 10321473 [PubMed - indexed for MEDLINE]

D'Souza I, Poorkaj P, Hong M, Nochlin D, Lee VM, Bird TD, Schellenberg GD.

Missense and silent tau gene mutations cause frontotemporal dementia with parkinsonism-chromosome 17 type, by affecting multiple alternative RNA splicing regulatory elements.
Proc Natl Acad Sci U S A. 1999 May 11;96(10):5598-603.
PMID: 10318930 [PubMed - indexed for MEDLINE]

Arrasate M, Perez M, Armas-Portela R, Avila J.
Polymerization of tau peptides into fibrillar structures. The effect of FTDP-17 mutations.
FEBS Lett. 1999 Mar 5;446(1):199-202.
PMID: 10100642 [PubMed - indexed for MEDLINE]